Predicting Snow-Cover and Frozen Ground Impacts on Large Basin Runoff: Developing Appropriate Model Complexity

Nan Wu[1,2,3,6], Ke Zhang[1,2,3,4,5,*], Amir Naghibi[6], Hossein Hashemi[6], Zhongrui Ning[2,3,6], Qinuo Zhang[1], Xuejun Yi[7], Haijun Wang[7], Wei Liu[7], Wei Gao[7], Jerker Jarsjö[8]

[1]The National Key Laboratory of Water Disaster Prevention, Hohai University, Nanjing, Jiangsu, 210024, China

[2]Yangtze Institute for Conservation and Development, Hohai University, Nanjing, Jiangsu, 210024, China

[3]College of Hydrology and Water Resources, Hohai University, Nanjing, Jiangsu, 210024, China

[4]China Meteorological Administration Hydro-Meteorology Key Laboratory, Hohai University, Nanjing, Jiangsu, 210024, China

[5]Key Laboratory of Water Big Data Technology of Ministry of Water Resources, Hohai University, Nanjing, Jiangsu, 210024, China

[6]Division of Water Resources Engineering, LTH, Lund University, Lund, 22100, Sweden

[7]Hydrological Center of Shandong Province, Jinan, Shandong, 250002, China

[8]Department of Physical Geography, Stockholm University, Stockholm, 10691, Sweden

Corresponding author: Ke Zhang (kzhang@hhu.edu.cn)

Abstract. In cold regions, snow and frozen ground can significantly influence hydrological processes, yet understanding is limited by insufficient observation data, in particular at large scales. To advance process understanding and capabilities of modeling large basin runoff in cold regions, we enhanced the existing Grid Xinanjiang (GXAJ) model framework by developing i) the Grid Xinanjiang-Snow cover model (GXAJ-S), incorporating snowmelt processes, and ii) the Grid Xinanjiang-Snow cover-Seasonally Frozen ground model (GXAJ-S-SF), which accounts for both snowmelt and freeze-thaw cycles. These models were calibrated using daily runoff data (2000–2010) and snow depth data (for the snowmelt process) to simulate runoff (2011–2018) in the middle and upper reaches of the extensive Yalong River basin, a region characterized by complex topography and a seasonally cold climate on the Qinghai-Tibet Plateau. The results highlight the importance of considering both snowmelt and frozen ground processes, as demonstrated by the significantly better performance of the GXAJ-S-SF model compared to the other variants. Specifically, the GXAJ-S-SF model showed that the presence of seasonally frozen ground (SFG) increased surface water runoff (by 39–77% compared to models neglecting SFG) during cold months, while reducing interflow, groundwater runoff, and soil evapotranspiration. These findings emphasize the significant hydrological impacts of SFG on large-basin runoff generation in mountainous areas. The flexible design of the snow and frozen ground components allows for their

integration into other hydrological models, providing a valuable tool for improving hydro-climatic assessments and predictions in cold mountainous regions. This approach is particularly relevant for assessing downstream water resource impacts under climate-driven changes in SFG.

Keywords: Frozen ground, Snow, Hydrological Modeling, Cold Regions. Climate change

1. Introduction

Seasonally Frozen Ground (SFG) has significant implications for the energy balance and water equilibrium of the land surface, which in turn affects ecosystems, hydrologic processes, soil properties, and biological activity worldwide. Seasonal freezing occurs across extensive areas, with approximately 25% of the Northern Hemisphere's land surface experiencing seasonal topsoil freezing in permafrost regions, i.e., the active layer, and an additional 25% outside the permafrost zone (Zhang et al., 2003). While the hydrological impacts of permafrost thaw and active layer changes have been extensively investigated over the past decade (Ford and Frauenfeld, 2016; Streletskiy et al., 2015), the hydrological impacts of SFG in permafrost-free regions have received less attention (Ala-Aho et al., 2021). The hydrological response to SFG is controversial and appears to be highly site- and time-specific (Appels et al., 2018). A systematic review by Ala-Aho et al. (2021) concluded that the impact of SGF on runoff processes is profound in many small-scale applications. However, large knowledge gaps remain, not least regarding the complex and less clear responses on larger scales for which the presence and absence of SFG may show considerable spatial variation. The possible, spatially

complex impacts of SFG on runoff in large basins may furthermore vary considerably within the year (Song et al., 2022). Shiklomanov (2012) similarly noted that despite the large scale and significant importance of SFG in cold regions, it has not received much attention due to the lack of long-term observational time series. Additionally, climate change is expected to alter frozen ground conditions and extent (Wang et al., 2019), increasing the frequency of freeze-thaw events in cold regions (Venäläinen et al., 2001). Thus, understanding the hydrological impacts of SFG under a warming climate, where permafrost is being transformed into SFG, is becoming increasingly important.

It is generally accepted that frozen ground, whether seasonally frozen or permafrost, constrains hydrological interactions to some extent. However, the hydrological response within permafrost regions differs significantly from areas where only the surface soil freezes seasonally. Permafrost extends deeply into the subsurface, impeding or even completely preventing deep groundwater runoff (Walvoord et al., 2012), leading to shallow groundwater runoff and rapid surface water runoff during snowmelt if the active layer of permafrost has not yet thawed (Hinzman et al., 1991). In contrast, the effects of SFG typically remain shallow in depth, increasing surface water runoff and reducing groundwater recharge during snowmelt if the topsoil is frozen (Ireson et al., 2013). This suggests that SFG disrupts surface-subsurface hydraulic connectivity in winter and spring while increasing hillslope runoff into the stream channels (Covino, 2017). This study focuses on SFD, which, at the regional scale, can serve as a crucial indicator of climate change and frozen ground conditions in cold regions.

SFG regions generally experience seasonal snow cover, which significantly influences the

soil freeze-thaw process. Due to the low thermal conductivity, high latent heat of melting, and high albedo of snow, changes in snow cover substantially alter the impact of air temperature on the thermal state of the soil (Goncharova et al., 2019), thereby affecting the soil freeze-thaw dynamics (Biskaborn et al., 2019). In areas of thin or transient snow cover in the SFG regions, thermal coupling between the ground and the atmosphere is more likely to increase the frequency and intensity of soil freezing while potentially reducing the duration of the freeze (Fuss et al., 2016). Consequently, soil in these regions may freeze more frequently and deeply but thaw more quickly due to weaker snowpack insulation. The seasonal effect of deep snowpack on ground temperatures depends on the thermal history of the ground, air temperature, and solar radiation that isolates the ground from the atmosphere (Maurer and Bowling, 2014). In a warming climate, a decrease in late-season snowpack may lead to increased soil freezing (Hardy et al., 2001). This phenomenon, termed "soil cooling in a warm world" (Groffman et al., 2001), emphasizes the complex effects of climate change on soil freezing and thawing processes. Therefore, the hydrological impacts of snow and SFG should be considered together as the two processes interact (Qi et al., 2019).

Hydrological processes associated with SFG and snow cover, including changes in soil moisture content and runoff component contributions, can be quantitatively simulated using process-based hydrological models (Gao et al., 2022; Qi et al., 2019). Physical process-based cold regions hydrological models such as the Geomorphology-Based Eco-Hydrological Model (GBEHM) (Yang et al., 2015), the Water and Energy Budget-based Distributed Hydrological Model (WEB-DHM) (Wang et al., 2009), the Variable Infiltration Capacity (VIC) model (Liang

et al., 1996), and the Cold Region Hydrological Model (CRHM) (Pomeroy et al., 2007) have been developed to assess various hydrological impacts of SFG and snow cover (Jafarov et al., 2018; Qi et al., 2016; Walvoord et al., 2019). While these models offer rigorous physical interpretations, they require a number of high-quality input data, and are hindered by parameterization complexities that induce simulation uncertainties (Gao et al., 2018), and exhibit slow computational speeds. Moreover, challenging climate and environmental conditions in cold regions pose difficulties for field observations, exacerbating local parameterization challenges. Conventional hydrological models such as SWAT (Arnold et al., 1995), HBV model (Krysanova et al., 1999), TOPMODEL (Beven and Kirkby, 1979), and Xinanjiang model (Zhao, 1984) predominantly focus on soil moisture conditions, neglecting the impacts of snowmelt and soil freeze-thaw processes. However, the soil freeze-thaw cycle traverses runoff processes, including infiltration, evaporation, and water migration, constituting a pivotal aspect of the hydrological cycle in cold regions (Guo et al., 2022). Although efforts have been made to integrate soil freeze-thaw processes into hydrological models (Ahmed et al., 2022; Huelsmann et al., 2015; Kalantari et al., 2015), most existing approaches, whether traditional or physical, rarely consider the impacts of snow and SFG simultaneously. There is also a lack of quantitative studies on the mechanisms by which snow and SFG affect hydrological processes. Furthermore, snow cover and SFG exhibit significant spatiotemporal heterogeneity and are influenced by numerous interconnected factors. The translation of point/slope-scale frozen processes into their basin-scale hydrological implications remains largely unexplored (Gao et al., 2022).

The Tibetan Plateau, the source region for many major rivers in Asia, provides water for billions of people and downstream ecosystems, earning the title "Asian Water Tower" (Immerzeel et al., 2010). The cryosphere of the Tibetan Plateau, consisting primarily of snow, permafrost, and glaciers (Qi et al., 2019), is highly sensitive to climate change. Seasonal snow cover and frozen ground significantly influence the hydrological processes in cold alpine regions, exhibiting pronounced intra-annual regulatory effects (Gao et al., 2023). Consistent with that, Pomeroy et al. (2007) recommended considering the coupling of seasonal freeze-thaw cycles with precipitation (snowfall) as a potential primary control on hydrological processes. The Xinanjiang model and its derivatives are considered the most commonly used practical flood forecasting models in China (Yao et al., 2014), with significant experience accumulated in operational flood forecasting (Chen et al., 2023); However, its adaptability in cold regions is relatively poor because it does not account for the influence of snow cover and frozen ground on the hydrological process.

Departing from the Grid Xinanjiang model (GXAJ), the primary objective of this study is to develop enhanced hydrological models at different levels of complexity, as represented by the snow model GXAJ-S and the snow-seasonally frozen ground model GXAJ-S-SF, to better simulate hydrological processes in cold regions. A main innovation is how the physical mechanisms of snowmelt and freeze-thaw cycles are coupled in the model. This is done in a way that enables quantitative analyses of the impacts of snowmelt and frozen ground on runoff, soil moisture dynamics and evapotranspiration while still keeping model complexity relatively low as compared to many physical process-based cold region models. Furthermore, in the light

of the above-mentioned considerable knowledge gaps on large-scale impacts of SFG on runoff, an additional novel aspect of the manuscript is related to the performed systematic comparison between simplified models (having no combined snow-SFG extensions, or accounting for snow processes only) and extended models that account for combined impacts of snow and SFG. On the one hand, simpler models with fewer input parameters have a wider applicability, not least in data-poor regions. On the other hand, models must be complex enough to represent the governing processes with sufficient accuracy. We therefore expect that present systematic investigation regarding to which extent SFG processes play governing roles in large basin runoff can provide guidance on the necessary level of complexity in large basin model applications.

2. Methodology

2.1 Cold region runoff mechanisms

The critical importance of ground freezing in the runoff generation of cold regions lies in the transformation of pre-existing water in soil pores into ice, which inhibits vertical water connectivity (Ala-Aho et al., 2021). Consequently, in areas with frozen ground, runoff processes are influenced not only by precipitation and soil moisture but also by ground freezing conditions driven by temperature variations (Wang et al., 2017). Based on the dynamic changes associated with seasonal freeze-thaw cycles and snow accumulation-melt dynamics, the runoff generation process are divided into four stages (Guo et al., 2022): initial freezing stage (IFS), stable freezing with snow stage (SFS-S), initial thawing stage (ITS), and complete thawing stage (CTS) (Fig. 1).

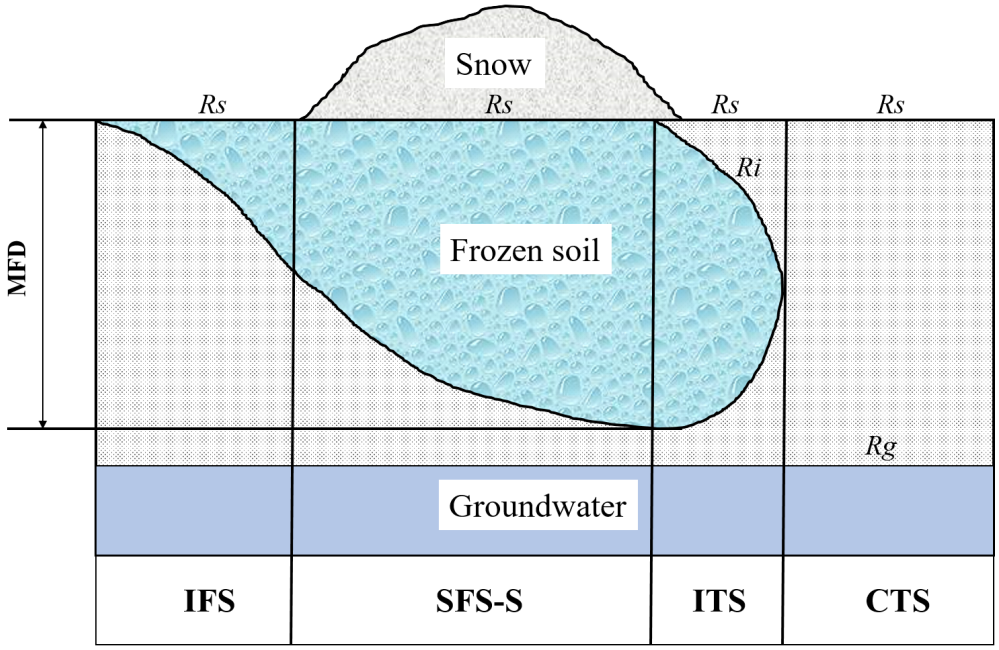

Figure 1. Runoff generation model in seasonally frozen ground/snow regions. R_s, R_i, and R_g represent surface water runoff, interflow, and groundwater runoff, respectively; MFD means maximum seasonal frozen ground depth.

i) During the IFS, temperatures are low, but no snowfall occurs. The ground freezes from the surface downwards (Thomas et al., 2009), significantly inhibiting the evaporation of soil moisture into the air and making it difficult for vegetation to absorb it. Due to the frozen surface layer, groundwater recharge is restricted. The precipitation during this stage mainly generates surface water runoff (R_s), which becomes the primary runoff component.

ii) Persistent low temperatures cause the depth of the frozen ground to increase while snow accumulates on the surface, maintaining the frozen state. The snow protects the cold ground from solar radiation despite warmer temperatures (Rush and Rajaram, 2022) until the snow completely melts. In the SFS-S, groundwater remains active beneath the frozen layer (Gao et al., 2022), soil evapotranspiration is nearly zero, and R_s generated by snowmelt or rainfall remains the main runoff component.

iii) During the ITS, as the temperature continues to rise and snow completely melts, the surface frozen ground begins to thaw, receiving substantial inputs from precipitation and snowmelt. During this stage, vegetation transpiration is very limited, and soil evaporation occurs only in the thawed surface layer. As a result, the surface layer easily saturates, generating saturation-excess runoff R_s. With increasing thaw depth, interflow (R_i) appears above the thaw front. Runoff during this stage primarily consist of a mix of R_s and R_i.

iv) In the CTS, the atmospheric and soil layers restore vertical connectivity. Increased rainfall events replenish groundwater, and evapotranspiration gradually increases. Runoff processes in this stage include R_s, R_i, and groundwater runoff (R_g).

In SFG/snow covered regions, precipitation and snowmelt are the primary sources of runoff. Temperature influences the seasonal freeze-thaw cycles of snow and frozen ground, and their interaction further affects soil water/ice content and evapotranspiration. Lower elevations generally experience higher temperatures compared to higher elevations, and south-facing slopes are generally warmer than north-facing slopes. Such local to regional temperature differences cause spatial variability in runoff, with transitions in runoff components across different freeze-thaw stages forming the fundamental runoff patterns in SFG regions.

2.2 Modeling approach

The GXAJ model (Yao et al., 2012) uses the concept of a saturated runoff mechanism, meaning that during rainfall, runoff will only occur once the soil water storage reaches the field capacity, with all incoming water being absorbed by the soil before that point. In the GXAJ model, the tension water storage capacity (W_M) (mm) of any grid cell is determined by the

geomorphological features and underlying surface conditions such as soil and vegetation (Stephens, 1996; U. S. Department of Algriculture, 2002). The potentially uneven distribution of W_M within a grid cell is not considered. The measured precipitation in the computation period is first adjusted by subtracting the corresponding period's evapotranspiration, vegetation canopy interception, and river precipitation. Then the upstream inflow is considered to check if it can replenish the soil moisture in the current grid cell. This results in an effective precipitation (P_e) that is used for runoff (R) calculation.

The runoff (R) from a grid cell is divided into three components: surface runoff R_s, interflow R_i, and groundwater runoff R_g. The GXAJ model assumes that the surface soil of the capillary zone is humus layer (determined by geomorphological features and soil, vegetation, and other surface conditions) (Li et al., 2004). The bottom of the humus layer is considered to be "relatively impermeable." A portion of the runoff generates R_i in the humus layer , while another part infiltrates further to produce R_g. When the free water in the humus layer becomes saturated, surface runoff occurs. Similarly, the uneven distribution of free water storage capacity (S_M) within the grid cell is not considered.

The GXAJ model calculates evapotranspiration using a three-layer model (Zhao and Wang, 1988). The soil is divided into upper, lower, and deep layers, with each layer having corresponding tension water storage capacities of W_{UM}, W_{LM} and W_{DM} (mm). When calculating actual evapotranspiration in a grid cell, canopy interception is evaporated based on its evapotranspiration capacity. If the interception is less than the evapotranspiration capacity, the three-layer model is used. The calculation principle of the three-layer evapotranspiration

model is as follows: The upper layer evaporates according to its capacity. If the upper layer's water content is insufficient, the remaining evapotranspiration capacity is used by the lower layer, which evaporates proportionally to the lower layer's water content and inversely to its water storage capacity. The ratio of the calculated lower layer evapotranspiration to the remaining evapotranspiration capacity must not be less than the deep-layer evapotranspiration coefficient (C). Otherwise, the deficit is replenished by the lower layer's water content, and when the lower layer is insufficient, it is supplemented by the deep layer's water content.

In summary, the GXAJ model partitions runoff into three components, i.e., R_s, R_i, and R_g, by calculating the tension water storage capacity (W_M) in the vadose zone and the free water storage capacity (S_M) in the humus layer (the spatial distribution is shown in Fig. S1). The W_M determines whether a grid cell generates runoff and the runoff volume (i.e., saturation-excess runoff), while the free water content of the surface soil differentiates the runoff components into R_i and R_g. When the free water content reaches saturation, R_s is produced, as illustrated in Fig. S2 (a). For actual evapotranspiration calculation, the soil within each grid cell is divided into three layers: upper, lower, and deep, with corresponding soil moisture and evapotranspiration labeled as W^u, W^l, and W^d, and E^u, E^l, and E^d, respectively, as shown in Fig. S2 (b). Confluence processes follow the calculation order between grids, sequentially routing various water sources to the watershed outlet. For details, refer to Yao et al. (2009).

However, the original GXAJ model does not account for the impacts of snow cover and freeze-thaw processes on runoff generation; studies have shown that this model is not suitable for seasonally cold regions (Yao et al., 2009, 2012). To address this, we here

introduce the snowmelt runoff process (SNOW17) and the freeze-thaw cycle processes into the GXAJ model, investigating if and to which extent the related expanded GXAJ-S model and GXAJ-S-SF model could better represent cold region hydrological processes (Fig. 2). Specifically, these processes explicitly account for the accumulation and melting of seasonal snow, as well as the spatiotemporal variations in soil freeze-thaw depth, using grid-based temperature and precipitation inputs. The SNOW17 model (Anderson, 1973) was chosen for snowmelt runoff calculation due to its minimal input requirements and clear representation of the most critical physical processes within the snowpack. Additionally, the Stefan equation was employed to predict seasonal soil freeze and thaw depths (Peng et al., 2017). The Stefan equation is widely used in conjunction with process-based models due to its simplicity and flexibility (Kurylyk, 2015).

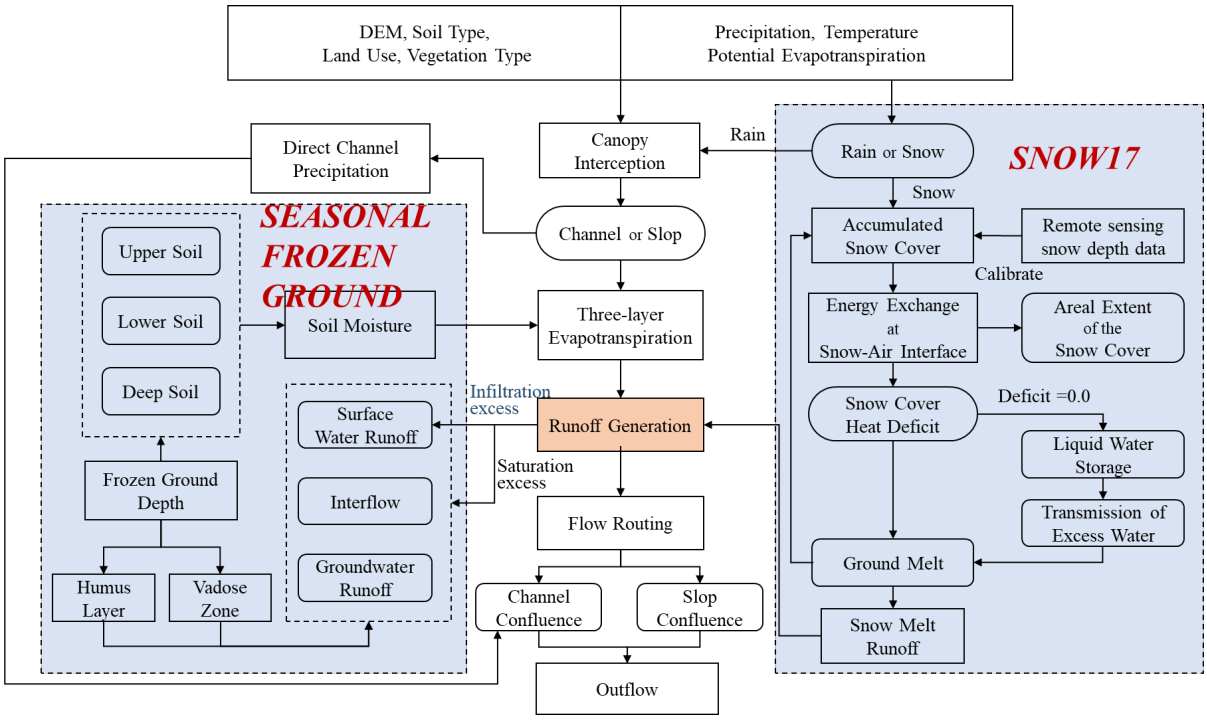

Figure 2. The schematic framework of the GXAJ-S-SF model.

2.2.1 Snow accumulation and melting runoff

Before snowfall occurs, if ground temperatures remain below freezing (0°C) for an extended period, the soil is subject to freezing (IFS) conditions. In related snow accumulation phases, as long as the snow cover remains relatively thin, most solar radiation is reflected by the snow cover due to its high albedo, while it yet does not insulate the ground, due to insufficient thickness. In contrast, thick snow covers, with their low thermal conductivities, can completely isolate the ground from the surrounding air temperature (Rush and Rajaram, 2022). Research has proposed a snow depth threshold of 30-40 cm (Hill, 2015), above which air temperature is not expected to affect ground temperature. At the lowest negative accumulated temperature, the maximum frozen depth is reached, with soil water retained as ice. As temperatures rise, the surface snow begins to melt first (Fig. S3).

The SNOW17 model (Anderson, 1973), developed as part of the National Weather Service river forecast system in the United States, was used for snowmelt prediction. The model description in this section is adapted from the latest references of the model (Anderson, 2006). The SNOW17 is an empirical lumped model that uses average daily temperature as the sole index to simulate snow accumulation, heat storage, snowmelt, liquid water retention, and meltwater transmission, determining energy exchange at the snow-air interface based on empirical relationships (He et al., 2011). The model outputs are snow depth and runoff time series. The snow accumulation and melting amount for each grid cell are calculated based on the snow-covered area. The SNOW17 model calculates snowmelt with and without rainfall, producing the total runoff during the snow cover period (O_s, mm).

The snow surface melting equation with rainfall is:

$$M_r = \sigma \cdot \Delta t_p \cdot [(T_a + 273)^4 - 273^4] + 0.0125 \cdot P \cdot f_r \cdot T_r + 8.5 \cdot UADJ \cdot ({}^{\Delta t_p}/_{6}) \cdot [(0.9 \cdot e_{sat} - 6.11) + 0.00057 \cdot P_a \cdot T_a] \quad (1)$$

where, M_r is the melt during rain-on-snow time intervals (mm), σ represents the Stefan-Boltzman constant ($6.12 \cdot 10^{-10}$ mm/°K/hr), Δt_p is the time interval of precipitation data (hour), T_a is the air temperature (°C), 273 represents 0°C on the Kelvin scale, f_r is the fraction of precipitation in the form of rain, T_r is the temperature of rain (°C), *UADJ* represents the average wind function (mm/mb/6 hr), and e_{sat} and P_a are saturated vapor pressure at T_a (mb) and atmospheric pressure (mb), respectively.

The snow surface melting equation without rainfall is:

$$M_{nr} = M_f \cdot (T_a - MBASE) \cdot \frac{\Delta t_p}{\Delta t_t} + 0.0125 \cdot P \cdot f_r \cdot T_r \quad (2)$$

where, M_{nr} is the melt during non-rain periods (mm), M_f is the melt factor (mm/°C/Δt_t), Δt_t is the time interval of temperature data (hours), and $MBASE$ is the base temperature (°C).

Most soil moisture exists in the form of solid ice, and the presence of frozen ground obstructs the infiltration of snowmelt water, resulting in surface water runoff (R_s^*, mm) as shown in Fig. S3 (a). In the presence of snow cover, soil moisture evaporation is generally impeded. The snow cover prevents the evaporation of moisture from the soil surface, while moisture on the snow surface is released into the atmosphere through sublimation (i.e., snow surface evaporation) as described by the SNOW17 model. Therefore, soil moisture evaporation is typically restricted under snow cover. Additionally, the frozen ground beneath the snow prevents soil moisture from being released into the atmosphere through evaporation, further

limiting soil moisture evaporation. The soil moisture status at this time is shown in the Fig. S3 (b).

2.2.2 Freeze-thaw process

The GXAJ-S-SF model employed the Stefan equation to estimate the approximate solution for the freeze-thaw depth. The Stefan equation is a temperature index-based freeze-thaw algorithm that assumes the sensible heat in soil freeze-thaw simulations can be neglected (Xie and Gough, 2013):

$$SFD = \sqrt{\frac{2 \cdot 86400 \cdot K_f \cdot F}{L \cdot \omega \cdot \rho}} \quad (3)$$

where SFD is the freeze-thaw depth (cm), K_f is the thermal conductivity of the soil ($W(mK)^{-1}$), F is the surface freezing-thawing index, with the freezing index being the cumulative negative ground temperature during freezing and the thawing index being the cumulative positive ground temperature during thawing. L is the latent heat of fusion for ice ($3.35\times10^5 Jkg^{-1}$), ω is the water content, and ρ is the bulk density of the soil ($kg\text{-}m^{-3}$). We set the thermal conductivity to $2W(mK)^{-1}$, the water content ω to 0.12 (as a fraction of dry soil weight), and the bulk density ρ to 1000 $kg\text{-}m^{-3}$ (Gao et al., 2022). Due to the lack of ground temperature data, a conversion factor was used to transform air temperature into ground temperature. During the freezing period, this factor was 0.6, while during thawing, it was assumed that ground temperature equaled air temperature (Gisnas et al., 2016).

To account for the insulating effect of snow cover on frozen ground, a threshold of 30 cm was used: if the snow depth exceeded 30 cm (Hill, 2015), the air temperature effect on frozen ground was ignored, regardless of whether low temperatures caused soil freezing or high

temperatures caused thawing. If the snow depth was below this threshold and the snow cover duration ranged between 60-140 days (Wu et al., 2024), the snow depth variable was added to the Stefan equation (Wang & Chen, 2022):

$$SFD^* = \sqrt{\frac{2 \cdot 86400 \cdot K_f \cdot F}{L \cdot \omega \cdot \rho}} / \sqrt[3]{ASD} \quad (4)$$

where *ASD* is the average snow depth.

In this study, the Stefan equation was driven by distributed temperature data, enabling us to simulate the soil freeze-thaw processes for each grid cell. The spatiotemporal variation of frozen soil depth affects runoff components, including soil water/ice, and soil evapotranspiration. We distinguish between four different possible type cases regarding associated runoff generation, each of which is associated with different modeling routines:

Case (a): When the surface soil is frozen, as shown in Fig. S4 (a), rainfall and snowmelt primarily generate surface water runoff (R_s^*). Soil water/ice content is shown in Fig. S5 (a). When the soil is in a frozen state, soil moisture cannot evaporate because the frozen ground forms an ice layer that prevents upward moisture evaporation.

Case (b): When the surface soil has thawed and the thawing depth is less than the depth of the humus layer (Fig. S4 (b)), the surface soil moisture exists in the form of liquid water. In this case, the thawed soil layer is considered to be the "new" vadose zone and the humus layer. The bottom of the thawed layer (impermeable layer) generates interflow (R_i^*), and since the thawed soil layer is relatively thin, surface saturation runoff (R_s^*) is easily generated:

$$R = P_e + W_0^* - W_M^* \quad (5)$$

$$R_i^* = K_i \times S^* \tag{6}$$

$$R_s^* = R + S^* - S_M^* \tag{7}$$

where P_e is the net rainfall during the period used for runoff calculation, mm; W_0^* is the initial soil moisture content of the thawed soil layer, mm; W_M^* is the tension water storage capacity of the thawed soil layer, S^* is the free water content in the thawed surface soil, K_i is the outflow coefficient of the surface soil free water content to the interflow, and S_M^* is the free water storage capacity in the thawed surface soil.

Among them, the variables with * represent relevant variables in the thaw layer, and their values are related to the temporal and spatial changes of the frozen soil depth:

$$W_0^* = \frac{(L_a - SFD^*)}{L_a} W_0 \tag{8}$$

$$S_0^* = \frac{(L_h - SFD^*)}{L_h} S_0 \tag{9}$$

$$W_M^* = \frac{(L_a - SFD^*)}{L_a} W_M = (L_a - SFD^*) \times (\theta_{fc} - \theta_{wp}) \tag{10}$$

$$S_M^* = \frac{(L_h - SFD^*)}{L_h} S_M = (L_h - SFD^*) \times (\theta_s - \theta_{fc}) \tag{11}$$

L_a and L_h are the thickness of the vadose zone and humus layer, respectively, which can be estimated by a soil moisture constant corresponding to the terrain index and soil type, mm; W_0, S_0, W_M, S_M are the corresponding water contents when there is no frozen soil (Yao et al., 2009).

At this time, there are two scenarios for soil moisture (Figs. S5 (b1) and S5 (b2)). As shown in Fig. S5 (b1), when the bottom of the thawed layer is in the upper soil, the upper soil moisture includes both liquid water W_w^u and frozen solid ice W_i^u. Evapotranspiration only affects the liquid water in the upper layer, while evapotranspiration in the lower and deep layers

is zero. When W_w^u is sufficient; the upper layer evapotranspiration E^u is:

$$E^u = K \times E_M \tag{12}$$

where K is the evapotranspiration coefficient, and E_M is the water surface evaporation during the period, mm.

When the bottom of the thawed layer reaches the lower soil layer (Fig. S5 (b2)), the entire upper soil is thawed, and the lower soil contains both solid and liquid water. At this time, the thawed lower layer is also affected by the evapotranspiration process. If the upper layer is dry and the lower thawed soil moisture content W_w^l is sufficient, the upper and lower layers are affected by the evapotranspiration, E^u and E^l, respectively:

$$E^u = K \times E_M \tag{13}$$

$$E^l = (K \times E_M - E^u) \times W_w^l / W_{LM}^* \tag{14}$$

where W_{LM}^* is the tension water storage capacity of the lower thawed soil layer (mm), which is related to the proportion of the lower thawed soil layer to the whole lower layer:

$$W_{LM}^* = \frac{(L_M - SFD^*)}{L_M} W_{LM} = (L_M - SFD_{LM}^*) \times (\theta_{fc} - \theta_{wp}) \tag{15}$$

L_M represents the depth of the lower layer soil, SFD_{LM}^* is the frozen depth of the lower layer soil.

Case (c): When the humus layer is completely thawed (Fig. S4 (c)), the thawed soil layer is considered to be the "new" vadose zone. According to the original GXAJ model's runoff generation theory, the bottom of the humus layer (relatively impermeable layer) generates R_i. At this time, there are two components of interflow: R_i and R_i^*. When the humus layer is saturated, R_s is generated. It is noteworthy that no groundwater runoff is generated throughout

the frozen soil period.

$$R = P_e + W_0^* - W_M^* \tag{16}$$

$$R_i = K_i \times S \tag{17}$$

$$R_i^* = K_g \times S \tag{18}$$

$$R_s = R + S - S_M \tag{19}$$

where S is the free water content in the surface soil L_h, K_g is the outflow coefficient of S to groundwater runoff, S_M is the free water storage capacity of L_h.

Soil moisture is present in two scenarios, with the bottom of the thawed layer appearing in the lower soil (Fig. S5 (c1)) and the deep soil (Fig. S5 (c2)). The evapotranspiration calculation for the first scenario (Fig. S5 (c1)) is consistent with Fig. S5 (b2). When the bottom of the thawed layer deepens to the deep soil (Fig. S5 (c2)), if the soil moisture in the upper and lower layers is also insufficient, it is necessary to calculate the deep layer thawed soil evapotranspiration E^d:

$$E^u = K \times E_M \tag{20}$$

$$E^l = (K \times E_M - E^u) \times W_w^l / W_{LM} \tag{21}$$

$$E^d = C \times (K \times E_M - E^u) - E^l \tag{22}$$

where C is the deep-layer evapotranspiration coefficient.

Case (d): Until the frozen soil is completely thawed, as shown in Fig. S5 (d), runoff calculation is performed according to the original GXAJ model (Fig. S2).

2.2.3 Model parameters and calibration

The original GXAJ model (operating on a daily scale) comprises 18 parameters (Table 1),

of which 13 are spatially variable parameters estimated based on vegetation type, soil texture, and topographic attributes. The remaining 5 parameters are derived from relevant operational experience with the model. When the SNOW17 model is applied to a specific location, it has a total of 10 parameters (Table 2), of which 4 are major parameters that must be determined through calibration, although some guidelines can be used for initial estimates (Anderson, 2002). The other secondary parameters have less impact on the results and can be assigned values according to the climatic conditions of the simulated location, requiring little adjustment from their initial values.

390 **Table 1.** GXAJ model parameters and their descriptions.

Module	Parameter	Description	A prior estimate
Canopy interception	LAI_{max}	Maximum *LAI* for the vegetation in a year	From LDAS based on vegetation types
	h_{lc}	Height of vegetation (m)	From LDAS based on vegetation types
Channel precipitation	W_{ch}	Channel width within a cell (km)	On the basis of the analysis of measured cross sections
Evapotranspiration	W_{UM}	Tension water capacity of upper layer (mm)	On the basis of initial estimation of W_M
	W_{LM}	Tension water capacity of lower layer (mm)	On the basis of initial estimation of W_M
	C	Evapotranspiration coefficient of deeper layer	On the basis of *LAI* and h_{lc} of vegetation
	K	Ratio of potential evapotranspiration to pan evaporation	From literature
Runoff generation	W_M	Tension water capacity (mm)	Using θ_{fc}, θ_{wp} and vadose zone thickness
	θ_s	Saturated moisture content	From literature based on soil types
	θ_{fc}	Field capacity	From literature based on soil types
	θ_{wp}	Wilting point	From literature based on soil types
	S_M	Free water capacity (mm)	Using θ_s, θ_{fc} and humus layer thickness
	K_i	Outflow coefficient of free water storage to interflow	On the basis of soil properties
	K_g	Outflow coefficient of free water storage to groundwater	On the basis of soil properties
Flow routing	C_i	Recession constant of interflow storage	From literature
	C_g	Recession constant of groundwater storage	From literature
	C_s	Recession constant in the lag and route technique	From literature
	L_{ag}	Lag time	From literature

Table 2. SNOW17 model parameters and their descriptions.

	Parameter	Description	Prior range
Major parameters	SCF	Snow correction factor, or gage catch deficiency adjustment factor	0.7 - 1.6
	$MFMAX$	Maximum solar melt factor during non-rain periods, assumed to occur on June 21 (mm·℃-1·6hr-1)	0.5 - 2.0
	$MFMIN$	Minimum solar melt factor during non-rain periods, assumed to occur on December 21 (mm·℃-1·6hr-1)	0.05 - 0.49
	$UADJ$	The average wind function during rain-on-snow periods (mm·mb^{-1})	0.03 - 0.19
	NMF	Maximum negative melt factor (mm·mb^{-1}·$6hr^{-1}$)	0.05 - 0.5
	$TIPM$	Antecedent temperature index parameter	0.01 - 1.0
	$PXTEMP$	The temperature that separates rain from snow (˚C)	-1 - 2
Minor parameters	$MBASE$	Base temperature for snowmelt computations during non-rain periods (˚C)	0 - 1.0
	$PLWHC$	Percent liquid water holding capacity for ripe snow (decimal fraction)	0.02 - 0.3
	$DAYGM$	Constant daily amount of melt which takes place at the snow-soil interface whenever there is a snow cover (mm·day-1)	-

To enhance the effectiveness of the model improvement and avoid the possibility that the introduction of additional parameters could potentially improve simulation results, the SNOW17 model was initially run independently. Remote sensing snow depth data (considered as "measured values") were used as input, and the parameters were adjusted to align the model-simulated snow depth with the "measured values," thereby determining the snow parameters for the study area. This approach allowed the integration of the SNOW17 model with the GXAJ model to form the GXAJ-S model for calculating snowmelt runoff in grid cells, ensuring that no new parameters were added to the GXAJ-S model compared to the GXAJ model. The freeze-thaw cycle processes employed empirical parameters (see Section 2.2.2), which were coupled with the GXAJ-S model to form the GXAJ-S-SF model. It is noteworthy that for the independent operation of the SNOW17 model to simulate snow depth (4 major parameters) and for runoff simulations using the three comparative models (GXAJ, GXAJ-S, and GXAJ-S-SF) with 5 empirical parameters, the parameter optimization algorithm, the SCE-UA method, was used (Duan et al., 1992). This method randomly selects a priori configurations within the allowed range of parameters and avoids local optimal solutions by running the optimization algorithm multiple times with different a priori configurations. By using this approach, we ensured that the parameter optimization process did not rely on a single set of prior configurations. It rather explored the parameter space to find the optimal solution, thus enhancing the robustness of the model results. Additionally, the optimization process focused only on the main parameters to avoid over-parameterization.

2.3 Model implementation and evaluations

2.3.1 Study area

The Yalong River is located in the southeastern part of the Tibetan Plateau and is the largest tributary of the Jinsha River. The main river stretches 1,571 km with a natural drop of 3,830 meters. Rich in hydroelectric resources, 21 hydropower stations are planned along the river, primarily concentrated in the downstream region. This study focuses on the mid-upper reaches of the Yalong River Basin (29.94°-34.21°N, 96.82°-101.63°E), with the Yajiang hydrological station serving as the outlet flow measurement (Fig. 3), covering an area of approximately 67,000 km². The elevation ranges from 2,500 to 5,900 meters, with a general south-north orientation with a high elevation in the northwest and low in the southeast, predominantly mountainous. Most precipitation occurs in summer, with limited snowfall in winter. Due to the complex terrain, meteorological observations in the study area are constrained. Seasonally frozen ground is widespread, with some areas containing sporadic permafrost (Ran et al., 2012). Seasonal snow significantly affects spring runoff, with about 50% of runoff directly fed by precipitation and the rest from glacier melt and groundwater (Wu et al., 2024). This pattern may change in the future due to global warming (Yao et al., 2022).

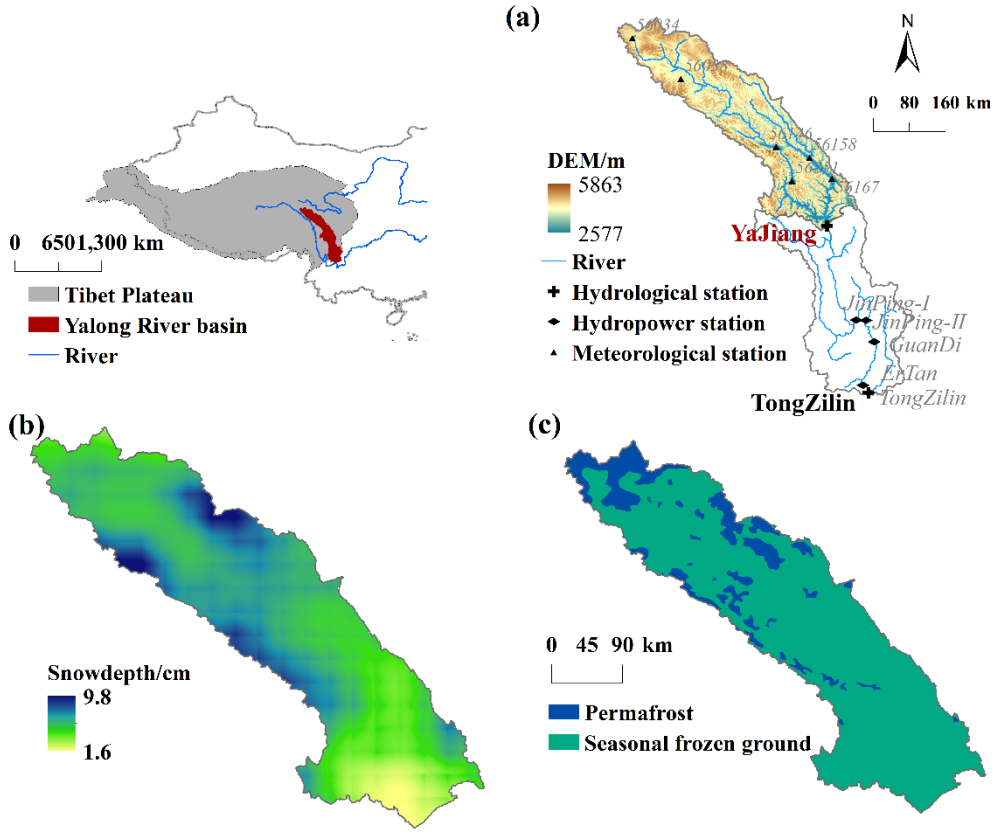

Figure 3. The mid-upper reaches of the Yalong River Basin in the southeastern Qinghai-Tibet Plateau, China, (a) topographic features, (b) annual average snow depth distribution, (c) seasonal frozen ground areas (https://doi.org/10.3972/westdc.0078.2013.db.).

2.3.2 Data collection, pre-processing and implementation

The data collection and description are presented in Table 3. Considering the computational efficiency of the model, the precision of precipitation, air temperature, snow depth, and all other data were resampled to 0.05°. The hydrological simulation performance of the original models (GXAJ and SNOW17) and the further developed models (GXAJ-S and GXAJ-S-SF) were evaluated in the mid-upper reaches of the Yalong River Basin. First, the SNOW17 model was calibrated (2000-2010) and validated (2011-2018) using remote sensing snow depth data to determine snowmelt parameters, with the freeze-thaw processes determined

through empirical formulas. Then, the developed models GXAJ-S and GXAJ-S-SF were used to simulate runoff during the same period, focusing on the snowmelt runoff period from March to June, and compared with the original GXAJ model. The impact of the two components (SNOW17 and SFG) on the runoff process, including runoff sources, components, and evapotranspiration, was also analyzed. Various statistical criteria, including Nash-Sutcliffe Efficiency (NSE), BIAS, Relative Error (RE), and Root Mean Squared Error (RMSE), were used to evaluate model performance. These criteria are defined in equations S1-S4.

Table 3. Data collection and description.

Data	Spatial resolution	Source	Description
Runoff	-	China Hydrology Yearbook from Ministry of Water Resources of China (http://www.mwr.gov.cn/) .	Daily runoff data (2000-2018) at the Yajiang hydrological station
Precipitation and air temperature	0.05°× 0.05°	China Meteorological Administration (CMA, http://data.cma.cn)	Precipitation and air temperature at meteorological stations were interpolated to 0.05° and corrected by post-processing analysis.
Ground temperature	-	China Meteorological Administration (CMA, http://data.cma.cn)	Site data
Potential evapotranspiration	0.25°×0.25°	-	Potential evapotranspiration was estimated using the Penman-Monteith model (Allen et al., 1998)
Atmospheric pressure, relative humidity, and sunshine duration	0.25°×0.25°	CN05.1 dataset (New et al., 2000)	Daily data (1961-2020), based on site data
Snow depth	0.05°× 0.05°	National Tibetan Plateau Data Center	Refer to (Yan et al., 2022)
Digital Elevation Model	1km×1km	U.S. Geological Survey (USGS) (GTOPO30)	https://www.usgs.gov/centers/eros/science/usgs-eros-archive-digital-elevation-global-30-arc-second-elevation-gtopo30
Vegetation cover	1km×1km	University of Maryland	Refer to (Potapov et al., 2022)
Soil type	10km×10km	Food and Agriculture Organization	Refer to (Fischer et al., 2008)
Maximum thickness of seasonally frozen ground	1km×1km	National Tibetan Plateau Data Center (https://cstr.cn/18406.11.Cryos.tpdc.300955)	Maximum thickness of seasonally frozen ground every 10 years from 1961 to 2020 was simulated using the Stefan equation based on remote sensing surface temperature data

3. Results

3.1 Simulation of snow accumulation and freeze-thaw process

At the basin scale, the SNOW17 model was first applied to determine the model parameters. The average daily snow depth simulated during the calibration period (2000-2010) and the validation period (2011-2018) was compared with remote sensing data. As shown in Fig. 4, the simulated snow depth closely followed the trend observed in the remote sensing data. Although the model slightly overestimated snow depth overall, it demonstrated reasonable accuracy in capturing the dynamics of snow depth. The model performed better during the validation period (RMSE = 1.6 cm, BIAS = 0.3 cm) compared to the calibration period (RMSE = 2.1 cm, BIAS = 0.9 cm). The model simulation error is relatively large when the snow depth is high, which may be attributed to a more complex snow melting process under deep snow conditions. Shallower snow depths may reduce errors related to model simplifications of complex snowmelt process under deep snow conditions, thereby improving the simulation accuracy. This may also be the reason why the simulation accuracy is higher in the validation period (shallower snow depth) than in the calibration period (deeper snow depth). The trend lines in Fig. 4 indicate a declining trend in snow depth from 2000 to 2018 in the mid-upper reaches of the Yalong River Basin, which is evident in both the remote sensing data and the model simulation results. Overall, the SNOW17 model showed satisfactorily simulations results of snow depth.

The Stefan empirical formula was used to calculate the seasonal freeze-thaw depth changes of the study area (Fig. 5). The results show that the maximum frozen depth was approximately 1.4 m. Freezing started at the end of September, the maximum depth was

reached by the end of March, and complete thawing occurred by the end of May. The accuracy in simulating the initial freeze and initial thaw dates was validated against ground temperature data from meteorological stations within the basin (Fig. S6). The spatial distribution of the average maximum frozen ground depth simulated in this study (2000-2018) was further compared with the dataset from National Tibetan Plateau Data Center (2000-2020) (Table 3, bottom row; Fig. S7). The frozen soil depth distribution in this study was obtained by the Stefan formula based on the station temperature interpolation. Therefore, its spatial distribution is relatively smooth. In both cases, the frozen soil depth showed the characteristics of deeper upstream and shallower downstream river areas in spatial distribution, and the numerical magnitude was similar, with a correlation coefficient as high as 0.89. These results provide strong support for the soil freeze-thaw results obtained by the GXAJ-S-SF model in this study. Besides, the trend from 2000 to 2018 showed a decreasing frozen depth, consistent with the snow accumulation and melting patterns (Fig. 4).

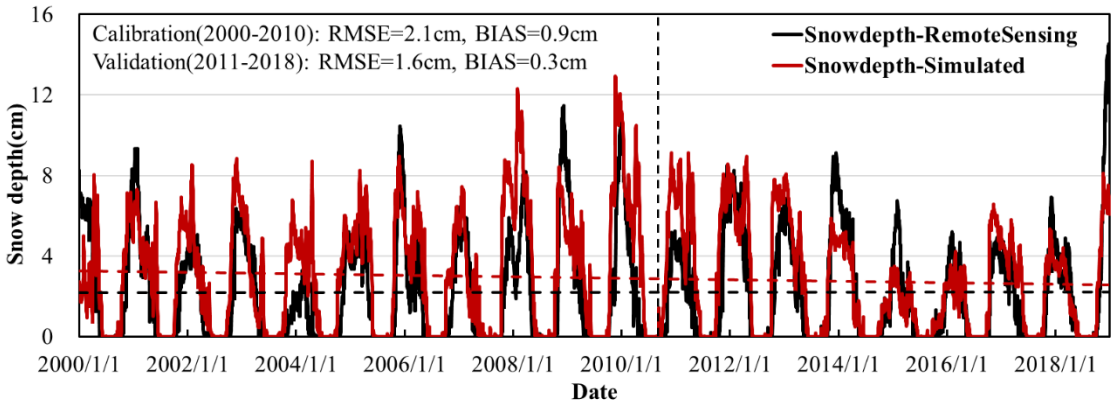

Figure 4. Comparison of simulated and observed basin-average snow depth in the Yalong River Basin during the calibration (2000-2010) and validation (2011-2018) periods, and the dashed lines represent the trend of snow depth.

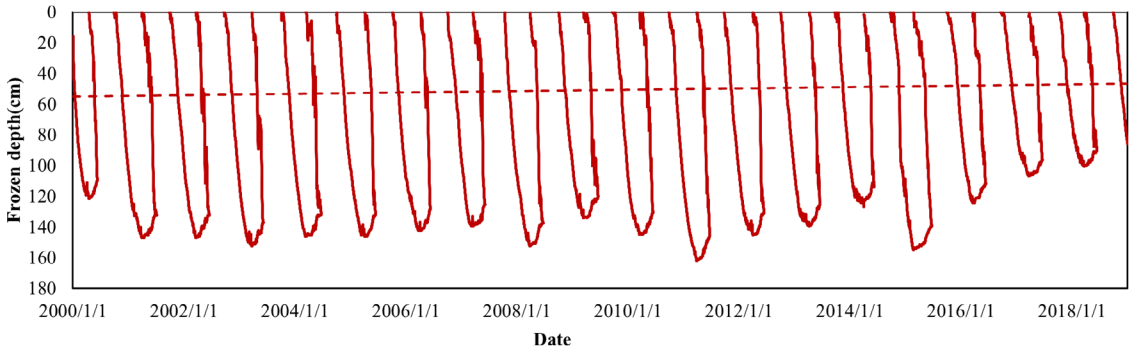

Figure 5. Seasonal freeze-thaw depth changes calculated using the Stefan empirical formula in the study area, and the dashed lines represent the trend of frozen depth.

To further illustrate impacts of freeze-thaw processes, Fig. 6 shows the annual variation of basin-average snow depth, frozen ground, effective humus layer, effective vadose zone, and soil water/ice content in 2001. The figure shows that the formation of frozen ground preceded the occurrence of snow. In particular, during periods of little or shallow snow depth (October–December), the rate of ground freezing was relatively fast. However, as snow depth increased (enhancing its insulating effect), the freezing rate gradually slowed down. Snow depth reached its maximum value (approximately 9 cm) in February and then rapidly decreased to 3 cm. Only when the snow depth was small (below 1 cm) did the ground freeze begin to melt. Therefore, the ground freezing and thawing trends were closely aligned with changes in snow depth.

Moreover, Fig. 6(b) demonstrates that frozen ground significantly reduces the effective vadose zone of the Yalong River basin, particularly during cold months (October–December and January–May), with the humus layer even becoming entirely frozen. Fig. 6(c) further illustrates a notable increase in soil ice content due to ground freezing, as well as a corresponding decrease in soil water content. These solid-liquid transformation processes of the Yalong River basin hence exert a critical influence on the water storage capacity of the vadose zone, alters infiltration pathways, and consequently affects the partitioning of runoff

into surface water and groundwater components.

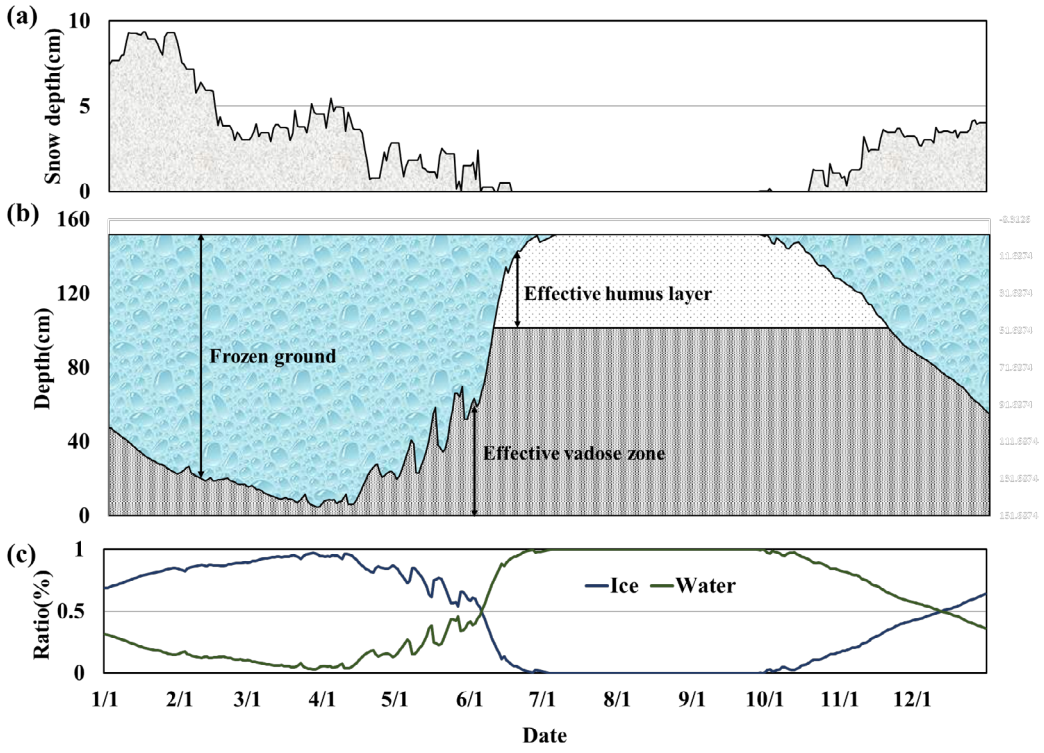

Figure 6. (a) Annual variation of basin-average snow depth; (b) impact of frozen ground on the basin-average depths of the effective vadose zone and humus layer; (c) basin-average ratio of water / ice content in the vadose zone, taking 2001 as an example

3.2 Calibration and validation of the streamflow

Fig. 7 (a) shows the simulated daily streamflow at the Yalong station of the GXAJ model from 2000 to 2018, without considering the effects of snow and seasonally frozen ground (SFG). The model did not distinguish between rainfall and snowfall, all incoming water was treated as rainfall. The model performed relatively well during both the calibration period (2000-2010) and the validation period (2010-2018), with NSE around 0.8. However, streamflow was often underestimated in winter and spring, which can be related to the impacts of frozen ground and snow. To further understand the model's performance in specific periods, the streamflow simulation results from March to June were analyzed separately (Fig. 7 (b)).

The results then showed that the GXAJ model had considerable inaccuracies in simulating spring snowmelt, especially during the validation period, where NSE decreased to 0.44 and RE reached -0.50. These metrics reflect that the GXAJ model calculated spring streamflow solely based on rainfall, failing to reflect the delayed effect of snowmelt on streamflow, which hence led to streamflow underestimation.

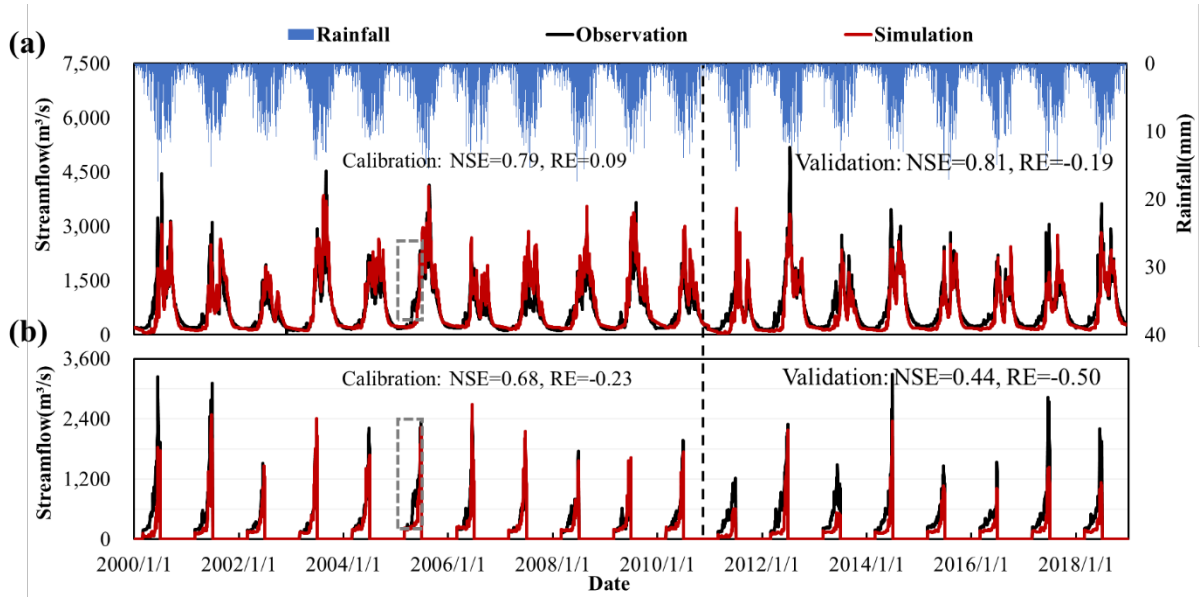

Figure 7. (a) Daily observed streamflow at the Yalong station and simulated streamflow by the GXAJ model during the calibration (2000-2010) and validation (2011-2018) periods, (b) with spring snowmelt from March to June highlighted (within dashed rectangle).

When snow cover effects were considered in the GXAJ-S model, the accuracy of daily streamflow simulation during 2000-2018 significantly improved (Fig. 8 (a)), especially during the calibration period (NSE=0.82, RE=0.05), indicating that a better performance of the GXAJ-S model in simulating snow accumulation and its hydrological effects, as compared to the original GXAJ model. However, as shown in Fig. 8 (b), the model still showed inaccuracies during the spring snowmelt period, particularly in the validation stage (NSE=0.68, RE=-0.36). The decrease in accuracy during the validation period may be partially related to changes in

applicability of model assumptions and parameter values between the calibration and validation periods. It probably also reflects that the model has not yet fully considered the interaction between snow and frozen ground on runoff, with the delayed water retention effect of frozen ground during the spring snowmelt period likely being a major source of error.

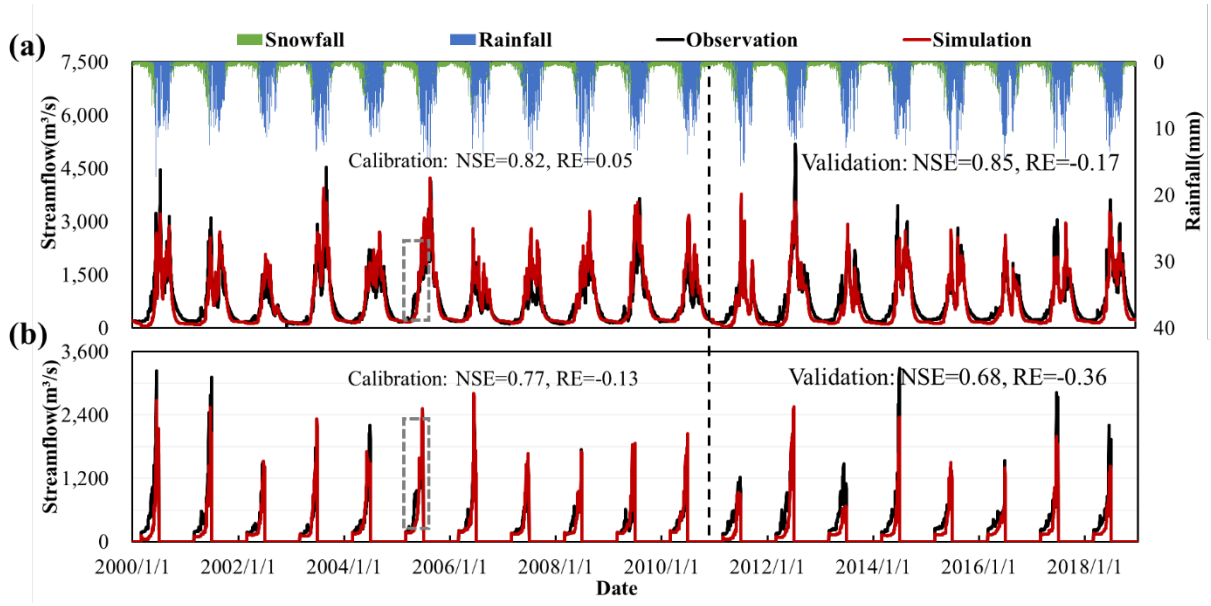

Figure 8. (a) Comparison of GXAJ-S model simulation results with observed values, (b) highlighting spring snowmelt from March to June.

Considering both snow cover and SFG effects, the GXAJ-S-SF model demonstrated excellent performance in overall daily runoff simulation (Fig. 9 (a)). The NSE values for both the calibration and validation periods exceeded 0.8, and the RE values were close to zero, indicating a high degree of fit between the model and observed runoff time series. Compared to the GXAJ-S model, the GXAJ-S-SF model was more accurate in simulating daily runoff, especially during the calibration period, showing higher accuracy. In simulating spring snowmelt runoff (Fig. 9 (b)), the GXAJ-S-SF model showed improvements over the previous models, particularly during the calibration phase, achieving higher accuracy. Although some underestimation remained in the validation period, the GXAJ-S-SF model demonstrated higher

accuracy compared to the other two models.

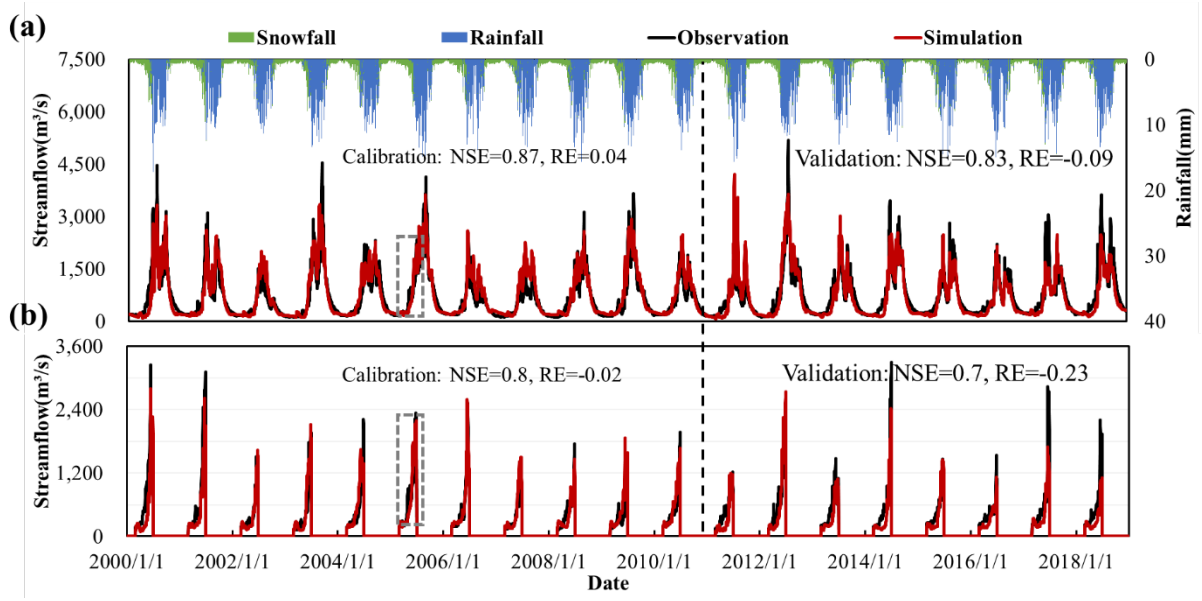

Figure 9. (a) Comparison of GXAJ-S-SF model simulation results with observed values, (b) highlighting spring snowmelt from March to June.

3.3 Model differences in simulated runoff components and soil evapotranspiration

Fig. 10 illustrates differences in the simulation of surface water runoff, interflow, and groundwater runoff among different models. The GXAJ and GXAJ-S models simultaneously reached the minimum percentage of interflow and maximum percentage of surface runoff in June and May, respectively, possibly due to the modelled soil saturation in both cases reaching relatively high values during the rainy summer season, thereby increasing surface runoff. Overall, the runoff components simulated by the GXAJ and GXAJ-S models were similar, with interflow accounting for the largest proportion (55-70%), followed by groundwater runoff (20-26%). The similarities between these two cases suggest that the omission (in GXAJ) or inclusion (in GXAJ-S) of snow processes in the modelling had a relatively limited impact on the simulated runoff dynamics. However, the GXAJ-S-SF model exhibited significant simulation differences. Fig. 10 (c) shows that during the cold months (January-March,

November-December), the proportion of surface water runoff increased significantly to 48-83%, mainly influenced by SFG (39-77%) as seen in Fig. 6b, while interflow and groundwater runoff decreased substantially. This was because SFG interrupted the connection between surface water and groundwater, preventing infiltration and leading to more surface water runoff. Additionally, the impact of SFG on interflow was most evident from March to May. As the surface soil thawed from top to bottom, the thawed soil layer tended to produce interflow. Groundwater runoff was hindered by frozen ground, remaining low during the cold season until frozen soil completely melted in summer, when groundwater runoff returned to its unfrozen state. This dynamic change indicates that SFG processes plays a critical role in regulating runoff composition over time. Moreover, SFG has a pronounced "decoupling effect" on surface runoff and groundwater runoff during cold months, interrupting their connection and restricting groundwater recharge and deep percolation.

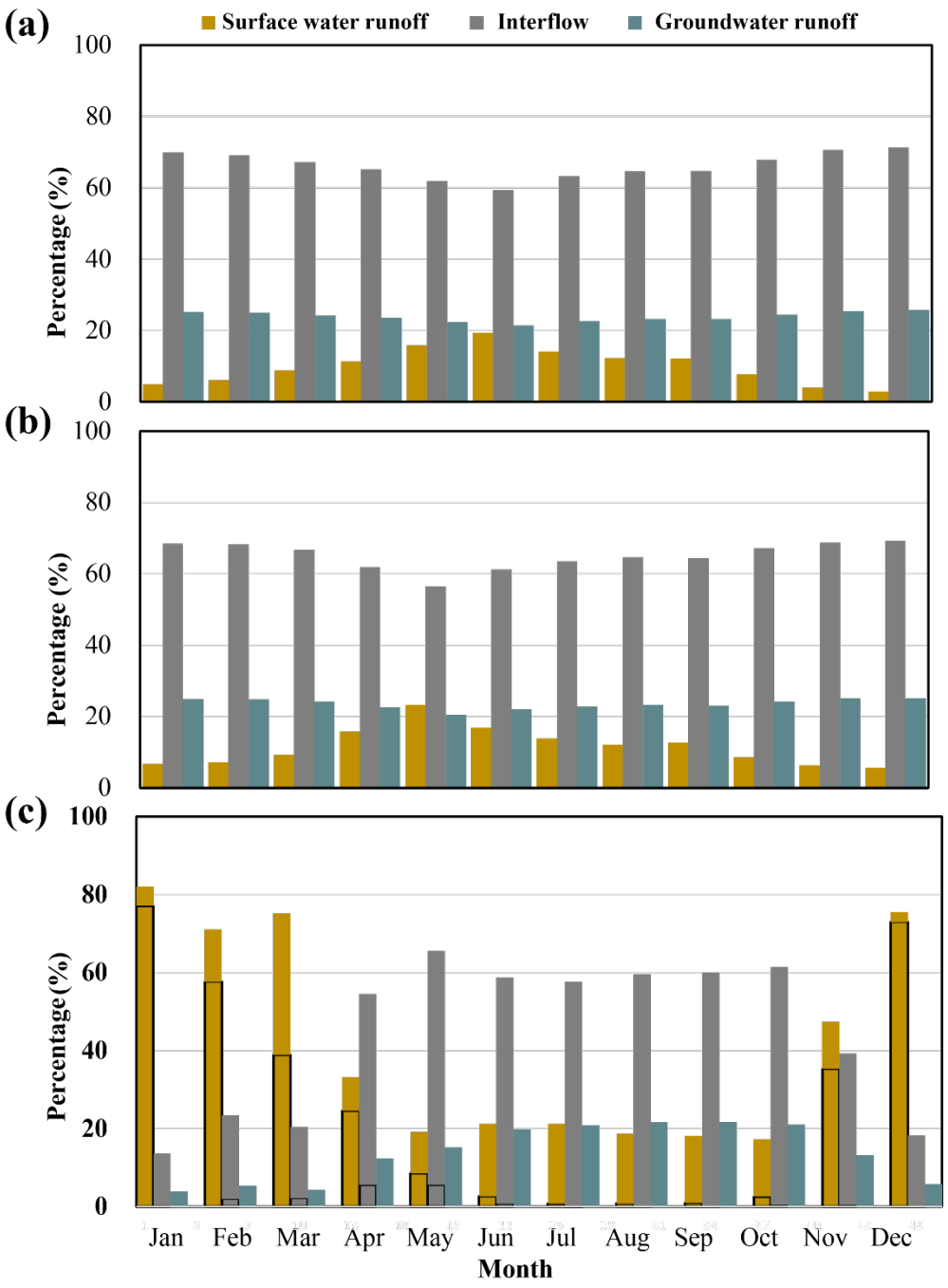

585 **Figure 10.** Comparison of simulated runoff components by models: (a) GXAJ, (b) GXAJ-S, and (c) GXAJ-S-SF, with the black box in (c) indicating runoff components influenced by SFG. The percentage of the y-axis represents the percent contribution of the considered runoff component (surface water runoff, interflow and groundwater runoff) to the total runoff.

The comparison of model outputs for soil evapotranspiration (Fig. 11) reveals that snow

590 and SFG significantly impact soil evapotranspiration, especially during the cold months. The

GXAJ model results exhibited some fluctuations in soil evapotranspiration during cold months, while the results of the GXAJ-S-SF model, which included the effects of snow and SFG, showed a significant reduction in soil evapotranspiration. This reduction can be attributed to two main mechanisms, the first one being that snow cover suppresses soil moisture evaporation, e.g. through sublimation processes, and the other one being that the formation of SFG creates a barrier within the soil, preventing upward evaporation of soil moisture. Consequently, the differences in output between the GXAJ-S-SF model and the GXAJ model highlights the significant regulatory effects of snow and SFG on soil evapotranspiration during the cold months, preserving soil moisture and reducing water loss. As expected, during the summer, the simulated results of the two models became very similar (as indicated by the dashed rectangle in Fig. 11 for the summer of 2010), reflecting a negligible basin-scale influence of any remaining high-altitude ground frost and snow.

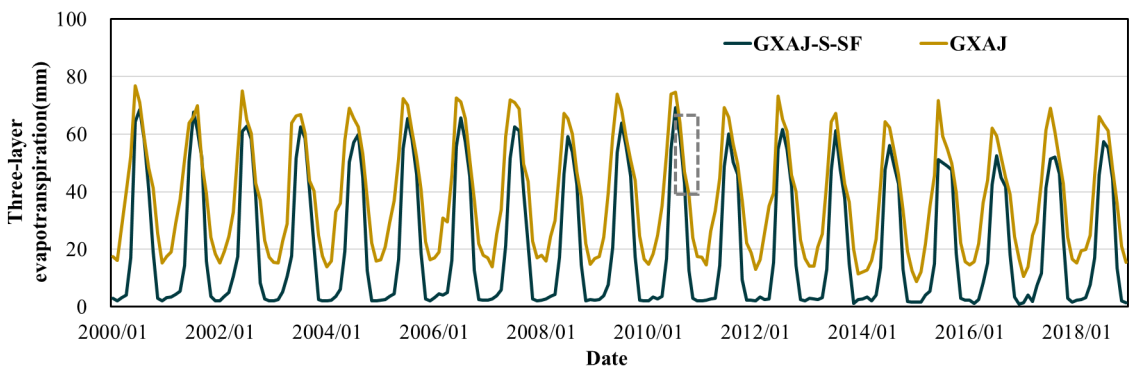

Figure 11. Simulated daily evapotranspiration series during the study period. The dashed rectangle represents 2010 summer evapotranspiration.

4. Discussion

4.1 Key limitations in hydrological models in relation to their process complexity

A limitation in the application of the GXAJ base model, which neglects impacts of snow

and ice, is related to the fact that the parameters of its modules are determined based on historical basin characteristics. Although such models without frozen ground components can, through appropriate calibration or optimization of parameters, in some cases successfully reproduce historical hydrological processes in cold regions under stable conditions (Li et al., 2011; Zhang et al., 2017), they may not be suitable for evaluating the consequences of future changes as their calibrated values do not represent new conditions of the basin, and as the model lacks physical representation of key drivers of change. Our study demonstrates that incorporating the effects of seasonally frozen ground (SFG) and snow into a basic model can provide robust and physically consistent results in simulating large-scale hydrological processes in cold regions, which can be particularly important for predicting hydrological impacts of future climate change scenarios. Key limitations in previous studies incorporating snow and seasonally frozen ground processes into hydrological models include taking 0°C as an assumed critical temperature for phase change, while neglecting the energy flux exchange between snow and soil layers, as for instance done in the VIC model (Liang et al., 1994). This potentially compromises simulation accuracy, particularly in regions where snow-frozen ground interactions are significant, such as areas with large seasonal variations in frozen ground depth. Similarly, while the SWAT model adjusts its parameters to accommodate permafrost conditions and introduces a new soil temperature module (Fabre et al., 2017), it does not account for the impact of snow depth on frozen ground and struggles to fully capture the complex and dynamic interactions between frozen ground and soil hydrological processes. Models such as the WEB-DHM (Qi et al., 2019), which employs enthalpy-based snow and frozen ground coupling, and the ATS model (Jafarov et al., 2018), have made substantial

progress in simulating multi-year snow and frozen ground dynamics. However, their high complexity and demanding data requirements limit their applicability in large-scale hydrological simulations.

In this context, while the here developed GXAJ-S-SF model does not rely on above-mentioned limitations of the VIC and SWAT models (as it accounts for the impact of snow depth variations on frozen ground and also captures multidimensional effects of snow-frozen ground coupling on hydrological processes) it still contains energy-related simplifications that makes it less dependent on extensive input data than e.g. the ATS model. In particular, the original lumped SNOW17 model (incorporated as a module in the GXAJ-S and GXAJ-S-SF model) was decentralized, and the energy exchange at the snow-atmosphere-soil interface was accurately simulated based on empirical relationships (He et al., 2011).

In complex mountainous cold regions, observation remains a bottleneck (Gao et al., 2022). Due to limitations in measured data on frozen soil and snow depth in the considered Yalong River basin, satellite-based snow depth data and ground temperature station data were used in the present study for calibration and verification. In particular, errors in remote sensing snow depth data (Yan et al., 2022; Zou et al., 2014) can propagate to the model output. However, previous studies have specifically investigated the here used remote sensing dataset for the Yalong River basin showing that its accuracy is high (Wu et al., 2024), which suggests that model errors should be relatively low. We also recognize that the use of surface temperature and maximum frozen ground depth to verify the freeze-thaw process introduces some uncertainty (Li et al., 2022), Since the GXAJ-S and GXAJ-S-SF model variants used the same temperature, snow and frozen ground data in the present simulations, they can be expected to

share similar data errors, However, due the non-linear nature of the modeled processes, such data errors may still not cancel completely when comparing different models. Nevertheless, observed differences in model performance between these models are mainly expected to reflect differences in model capabilities rather than differences in input datasets. Future work should focus on improving remote sensing data quality and exploring the long-term robustness of the model to further enhance performance and improve our understanding of the freeze-thaw processes in complex mountainous cold regions.

Hydrological modeling typically prioritizes model fitness, which in theory can be improved by introducing more fitting parameters. However, this study highlights differences that are due to addition of process-based modules (regarding snow and frozen ground). This implies that improvements in model fit and differences in associated model output (e.g. runoff and evapotranspiration) reflect how the considered snow and/ or frozen ground processes more concretely alter hydrological flows. This therefore increases the understanding of underlying hydrological processes (Gao et al., 2022) in large-scale applications such as the Yalong River basin that additionally has a complex topography with large elevation differences yielding high spatio-temporal heterogeneity in snowmelt and freeze-thaw cycles of soil.

4.2 The impact of seasonal frozen ground/snow

SFG is a thermal condition dependent on ground heat. As previously mentioned, it is clear that SFG in many cases has crucial impact locally, because when the ground freezes, ice blocks some previously water-filled soil pores, preventing water from flowing through those pores. This can impact the seasonal permeability of the vadose zone and groundwater recharge (Ge et al., 2011). However, frozen ground impacts on basin hydrology remains difficult to explore

(Gao et al., 2022), and its importance in different settings, as well as its general importance on larger scales is therefore relatively unknown (Ala-Aho et al., 2021). Present results for the spatially extensive Yalong River basin provided evidence of SFG processes indeed being important for the basin's large-scale runoff processes. This is because the here considered GXAJ-S-SF model, which simultaneously accounted for the impacts of snow and SFG, showed considerable enhancements in simulating different runoff components as compared with the GXAJ-S and GXAJ models, both of which did not consider SFG impacts.

Additionally, the impact of soil freeze-thaw cycles on the entire basin hydrological process varies across seasons (Fig. 6; Gao et al., 2023). Spring runoff mainly consists of surface water runoff and interflow, while summer thawing of frozen ground increases groundwater recharge (Huelsmann et al., 2015), which is consistent with the findings of this study (Fig.10). Ground freezing conditions are highly dependent on snow conditions, as snow has a low thermal conductivity and acts as an insulator. The depth of the snow is usually negatively correlated with ground freezing depth (Iwata et al., 2011). Therefore, despite sub-zero temperatures, thick snow cover in early winter can significantly reduce or even completely prevent the formation of ground freezing (Fig. 6; Iwata et al., 2018). More generally, the multi-model simulations of daily runoff processes therefore provided important insights into key factors governing basin hydrology under seasonal variations in cold regions.

Furthermore, the inhibitory effects of snow and SFG on soil evapotranspiration are evident, as reflected in the GXAJ-S-SF model's simulation results. The freeze-thaw process complicates soil moisture movement in the vadose zone. Within the frozen layer, moisture movement is minimal, resulting in negligible upward evaporation and almost zero recharge to groundwater

below. Above the freezing interface, water moves upward and evaporates, while gravitational water moves downward, accumulating and filling soil pores at the thawing interface (Fig. S4). This process results in the formation of a saturated layer above the frozen ground (Guo et al., 2022; Huelsmann et al., 2015; Ireson et al., 2013; Wang et al., 2017). As the thawing layer thickens, the vadose zone's thickness and water storage capacity increase, enhancing both evaporation and infiltration capabilities. This phenomenon indicates that during the freezing periods, evaporation rates are very low, as ice within the soil inhibits the movement of liquid water (Yu et al., 2018). Additionally, due to low winter temperatures, transpiration rates are also significantly reduced. These processes, including freeze-thaw dynamics, soil moisture movement, and the effects of snow and SFG on evapotranspiration, can influence the hydrological cycle and ecosystems by altering water availability and flow patterns. These effects, particularly during freeze-thaw periods, may lead to changes in water storage, infiltration, and runoff, which can alter regional water resource management and ecosystem resilience.

In addition, snowmelt runoff is a vital component of spring runoff in the Yalong River Basin, as further demonstrated in this study (Fig. S8). Snow cover varies with elevation, exhibiting significant spatiotemporal heterogeneity (Li et al., 2018). Under the backdrop of global warming, rising average temperatures are expected to affect the composition and duration of snow cover (Fig. S9; IPCC, 2021). Changes in snowmelt volume can influence downstream runoff, impacting water resource management and ecological balance. Incorporating the effects of snow into this study has improved the predictive accuracy of hydrological simulations for daily runoff and spring snowmelt runoff (Fig. 7, 8). Both remote

sensing data and model simulation results in this study showed a decreasing trend in snow/frozen depth from 2000 to 2018 (Figs. 4, 5). Winter snowmelt water typically infiltrates the upper soil layer, forming an almost impermeable "concrete frost" layer at the interface between the ground and snow layer upon refreezing (Dunne and Black, 1971). Due to warming, the ice content in SFG is denser, potentially altering the hydrological response of SFG during major spring snowmelt periods (Hardy et al., 2001). The snowfall process profoundly impacts ground thermal conditions, with some proposing that we might even see "colder soils in warmer climates" (Halim and Thomas, 2018). In summary, predicting future changes in SFG and its hydrological importance remains challenging due to the complex interactions between climate, land, water, ecosystems, and human activities. The hydrological relevance of SFG may increase due to factors such as reduced snow cover and changes in snow insulation capacity, more frequent freeze-thaw cycles, rain-on-snow events, and land cover changes (Ala-Aho et al., 2021). Such may therefore significantly impact the spatial and temporal availability of water resources in SFG regions.

This study quantitatively analyzed the impact of seasonal snow and frozen ground on hydrological processes based on the hydrological model, and its validity was confirmed not only by measured runoff but also by multi-source data, especially the trends in snow and frozen soil changes. Although our developed model has great application potential in other cold regions, it should be used cautiously without prior understanding of the modeling system. Snow and frozen ground are just part of the factors affecting cold-region hydrology, with other factors intertwined with frozen ground having significant impacts. Geological conditions, in particular, greatly affect frozen ground but have large spatial heterogeneity and are challenging to measure.

The empirical parameters of the SNOW17 model and Stefan equation have clear physical significance and have been validated by previous studies (Anderson, 2006; Ran et al., 2022; Zou et al., 2014). However, the soil and geology of mountainous basins are extremely complex and vary significantly across regions. This complexity introduces challenges in applying these models to different watersheds, requiring recalibration of their values. For instance, soil texture, moisture retention, and thermal properties can vary considerably, influencing the depth and dynamics of the seasonal frozen ground. Similarly, variations in topography, vegetation cover, and geological composition can impact runoff, infiltration, and evapotranspiration processes. Expanding the application of complex hydrological models therefore requires careful attention to local and regional variability in ambient conditions, but may also considerably increase the understanding of processes and the generalizability of the assumptions made.

5. Conclusions

The understanding of cold-region hydrology remains incomplete, primarily due to limited observational data, which also constrains quantitative analyses of water flows and water resources, especially in complex mountainous basins like the Tibetan Plateau. In this study, we compared runoff simulations from the original GXAJ model and two enhanced versions (GXAJ-S, which incorporates snowmelt, and GXAJ-S-SF, which additionally considers freeze-thaw processes) against measured daily runoff (2000–2018) obtained at the Yajiang discharge station in the Yalong River basin. The results showed that the GXAJ-S-SF model achieved the highest simulation accuracy, with significant improvements in NSE and RE for total runoff and runoff during snowmelt conditions. From a process perspective, the GXAJ-S-SF model revealed that the inclusion of seasonally frozen ground (SFG)—neglected in the other two

model versions—led to a notable increase in surface runoff (by 39–77% compared to the other models) during the cold months, while reducing interflow and groundwater runoff. The GXAJ-S-SF model also captured significant reductions in soil evapotranspiration due to the effects of snow and SFG processes. These findings underscore the substantial influence of SFG on large-basin hydrological processes, including impacts on surface water-groundwater partitioning and vertical (evaporative) water fluxes across the land surface in mountainous areas. The snow and SFG components developed in this study are designed with flexibility and adaptability, enabling seamless integration into other hydrological models beyond GXAJ. This capability offers a pathway to improve predictions of hydrological changes under climate warming, particularly in cold mountainous regions where SFG is expected to undergo significant alterations. Explicitly accounting for these dynamics could substantially enhance future assessments of hydro-climatic changes and their associated impacts on downstream water resources.

Declaration of Competing Interest

The authors declare that they have no known competing financial interests or personal relationships that could have appeared to influence the work reported in this paper.

Acknowledgments

This study was supported by the Fundamental Research Funds for the Central Universities of China (B220204014, B220203051, and B210204013) and the National Natural Science Foundation of China (51879067). The first author also received a grant from the China

Scholarship Council to study at Lund University in Sweden. The authors thank Ministry of Water Resources of China (http://www.mwr.gov.cn/) for providing the natural and observed streamflow, the China Meteorological Administration (CMA) for providing the climatic data (http://data.cma.cn/). The code and data used in this paper are available from the first author's GitHub repository (https://github.com/NanWu16/) or by contacting the corresponding author (kzhang@hhu.edu.cn).

References

Ahmed, N., Wang, G., Booij, M. J., Marhaento, H., Pordhan, F. A., Ali, S., Munir, S., and Hashmi, M. Z.-R.: Variations in hydrological variables using distributed hydrological model in permafrost environment, Ecol. Indic., 145, 109609, https://doi.org/10.1016/j.ecolind.2022.109609, 2022.

Ala-Aho, P., Autio, A., Bhattacharjee, J., Isokangas, E., Kujala, K., Marttila, H., Menberu, M., Merio, L.-J., Postila, H., Rauhala, A., Ronkanen, A.-K., Rossi, P. M., Saari, M., Haghighi, A. T., and Klove, B.: What conditions favor the influence of seasonally frozen ground on hydrological partitioning? A systematic review, Environ. Res. Lett., 16, 043008, https://doi.org/10.1088/1748-9326/abe82c, 2021.

Allen, R. G., Pereira, L. S., Raes, D., and Smith, M.: Crop evapotranspiration-Guidelines for computing crop water requirements-FAO Irrigation and drainage paper 56, Food and Agriculture Organization of the United Nations, Rome, 1998.

Anderson, E.: Calibration of Conceptual Hydrologic Models for Use in River Forecasting, US National Weather Service, Silver Spring, 2002.

Anderson, E. A.: National Weather Service river forecast system: Snow accumulation and ablation model, US Department of Commerce, National Oceanic and Atmospheric Administration, 1973.

Anderson, E. A.: Snow accumulation and ablation model–SNOW-17, US National Weather Service, Silver Spring, MD, 61, 2006.

Appels, W. M., Coles, A. E., and McDonnell, J. J.: Infiltration into frozen soil: From core-scale dynamics to hillslope-scale connectivity, Hydrol. Process., 32, 66–79, https://doi.org/10.1002/hyp.11399, 2018.

Arnold, J., Williams, J., and Maidment, D.: Continuous-Time Water and Sediment Routing Model for Large Basins, J. Hydraul. Eng.-ASCE, 121, 171–183, https://doi.org/10.1061/(ASCE)0733-9429(1995)121:2(171),

1995.

Beven, K. J. and Kirkby, M. J.: A physically based, variable contributing area model of basin hydrology, Hydrol. Sci. J.-J. Sci. Hydrol., 24, 43–69, https://doi.org/10.1080/02626667909491834, 1979.

Biskaborn, B. K., Smith, S. L., Noetzli, J., Matthes, H., Vieira, G., Streletskiy, D. A., Schoeneich, P., Romanovsky, V. E., Lewkowicz, A. G., Abramov, A., Allard, M., Boike, J., Cable, W. L., Christiansen, H. H., Delaloye, R., Diekmann, B., Drozdov, D., Etzelmueller, B., Grosse, G., Guglielmin, M., Ingeman-Nielsen, T., Isaksen, K., Ishikawa, M., Johansson, M., Johannsson, H., Joo, A., Kaverin, D., Kholodov, A., Konstantinov, P., Kroeger, T., Lambiel, C., Lanckman, J.-P., Luo, D., Malkova, G., Meiklejohn, I., Moskalenko, N., Oliva, M., Phillips, M., Ramos, M., Sannel, A. B. K., Sergeev, D., Seybold, C., Skryabin, P., Vasiliev, A., Wu, Q., Yoshikawa, K., Zheleznyak, M., and Lantuit, H.: Permafrost is warming at a global scale, Nat. Commun., 10, 264, https://doi.org/10.1038/s41467-018-08240-4, 2019.

Chen, X., Zhang, K., Luo, Y., Zhang, Q., Zhou, J., Fan, Y., Huang, P., Yao, C., Chao, L., and Bao, H.: A distributed hydrological model for semi-humid watersheds with a thick unsaturated zone under strong anthropogenic impacts: A case study in Haihe River Basin, J. Hydrol., 623, 129765, https://doi.org/10.1016/j.jhydrol.2023.129765, 2023.

Covino, T.: Hydrologic connectivity as a framework for understanding biogeochemical flux through watersheds and along fluvial networks, Geomorphology, 277, 133–144, https://doi.org/10.1016/j.geomorph.2016.09.030, 2017.

Duan, Q., Sorooshian, S., and Gupta, V.: Effective and Efficient Global Optimization for Conceptual Rainfall-Runoff Models, Water Resour. Res., 28, 1015–1031, https://doi.org/10.1029/91WR02985, 1992.

Dunne, T. and Black, R.: Runoff Processes During Snowmelt, Water Resour. Res., 7, 1160-, https://doi.org/10.1029/WR007i005p01160, 1971.

Fabre, C., Sauvage, S., Tananaev, N., Srinivasan, R., Teisserenc, R., and Perez, J. M. S.: Using Modeling Tools to Better Understand Permafrost Hydrology, Water, 9, 418, https://doi.org/10.3390/w9060418, 2017.

Fischer, G., Nachtergaele, F., Prieler, S., van Velthuizen, H. T., Verelst, L., and Wiberg, D.: Global Agro-ecological Zones Assessment for Agriculture, IIASA and FAO, Laxenburg, Austria and Rome, Italy., 2008.

Ford, T. W. and Frauenfeld, O. W.: Surface-Atmosphere Moisture Interactions in the Frozen Ground Regions of Eurasia, Sci Rep, 6, https://doi.org/10.1038/srep19163, 2016.

Fuss, C. B., Driscoll, C. T., Green, M. B., and Groffman, P. M.: Hydrologic flowpaths during snowmelt in forested headwater catchments under differing winter climatic and soil frost regimes, Hydrol. Process., 30,

4617–4632, https://doi.org/10.1002/hyp.10956, 2016.

Gao, B., Yang, D., Qin, Y., Wang, Y., Li, H., Zhang, Y., and Zhang, T.: Change in frozen soils and its effect on regional hydrology, upper Heihe basin, northeastern Qinghai-Tibetan Plateau, Cryosphere, 12, 657–673, https://doi.org/10.5194/tc-12-657-2018, 2018.

Gao, H., Ding, Y., Zhao, Q., Hrachowitz, M., and Savenije, H. H. G.: The importance of aspect for modelling the hydrological response in a glacier catchment in Central Asia, Hydrol. Process., 31, 2842–2859, https://doi.org/10.1002/hyp.11224, 2017.

Gao, H., Han, C., Chen, R., Feng, Z., Wang, K., Fenicia, F., and Savenije, H.: Frozen soil hydrological modeling for a mountainous catchment northeast of the Qinghai–Tibet Plateau, Hydrol. Earth Syst. Sci., 26, 4187–4208, https://doi.org/10.5194/hess-26-4187-2022, 2022.

Gao, H., Zhang, Z., Chen, H., Zhang, W., Xu, C., Yi, Y., Liu, J., and Xiao, Z.: Impacts of seasonally frozen soil hydrothermal dynamics on the watershed hydrological processes inferred from a spatially distributed numerical modelling approach, J. Hydrol., 624, 129947, https://doi.org/10.1016/j.jhydrol.2023.129947, 2023.

Ge, S., McKenzie, J., Voss, C., and Wu, Q.: Exchange of groundwater and surface-water mediated by permafrost response to seasonal and long term air temperature variation, Geophys. Res. Lett., 38, L14402, https://doi.org/10.1029/2011GL047911, 2011.

Gisnas, K., Westermann, S., Schuler, T. V., Melvold, K., and Etzelmuller, B.: Small-scale variation of snow in a regional permafrost model, Cryosphere, 10, 1201–1215, https://doi.org/10.5194/tc-10-1201-2016, 2016.

Goncharova, O. Y., Matyshak, G. V., Epstein, H. E., Sefilian, A. R., and Bobrik, A. A.: Influence of snow cover on soil temperatures: Meso- and micro-scale topographic effects (a case study from the northern West Siberia discontinuous permafrost zone), Catena, 183, 104224, https://doi.org/10.1016/j.catena.2019.104224, 2019.

Groffman, P. M., Driscoll, C. T., Fahey, T. J., Hardy, J. P., Fitzhugh, R. D., and Tierney, G. L.: Colder soils in a warmer world: A snow manipulation study in a northern hardwood forest ecosystem, Biogeochemistry, 56, 135–150, https://doi.org/10.1023/A:1013039830323, 2001.

Guo, D. and Wang, H.: CMIP5 permafrost degradation projection: A comparison among different regions, J. Geophys. Res.-Atmos., 121, 4499–4517, https://doi.org/10.1002/2015JD024108, 2016.

Guo, L., Huang, K., Wang, G., and Lin, S.: Development and evaluation of temperature-induced variable source area runoff generation model, J. Hydrol., 610, 127894, https://doi.org/10.1016/j.jhydrol.2022.127894,

2022.

Halim, M. A. and Thomas, S. C.: A proxy-year analysis shows reduced soil temperatures with climate warming in boreal forest, Sci Rep, 8, 16859, https://doi.org/10.1038/s41598-018-35213-w, 2018.

Han, P., Long, D., Han, Z., Du, M., Dai, L., and Hao, X.: Improved understanding of snowmelt runoff from the headwaters of China's Yangtze River using remotely sensed snow products and hydrological modeling, Remote Sens. Environ., 224, 44–59, https://doi.org/10.1016/j.rse.2019.01.041, 2019.

Hardy, J. P., Groffman, P. M., Fitzhugh, R. D., Henry, K. S., Welman, A. T., Demers, J. D., Fahey, T. J., Driscoll, C. T., Tierney, G. L., and Nolan, S.: Snow depth manipulation and its influence on soil frost and water dynamics in a northern hardwood forest, Biogeochemistry, 56, 151–174, https://doi.org/10.1023/A:1013036803050, 2001.

He, M., Hogue, T. S., Franz, K. J., Margulis, S. A., and Vrugt, J. A.: Characterizing parameter sensitivity and uncertainty for a snow model across hydroclimatic regimes, Adv. Water Resour., 34, 114–127, https://doi.org/10.1016/j.advwatres.2010.10.002, 2011.

Hill, A.: Controls on Snowmelt Partitioning to Surface and Groundwater Flow, 2015 AGU Fall Meeting, 2015.

Hinzman, L., Kane, D., Gieck, R., and Everett, K.: Hydrologic and Thermal-Properties of the Active Layer in the Alaskan Arctic, Cold Reg. Sci. Tech., 19, 95–110, https://doi.org/10.1016/0165-232X(91)90001-W, 1991.

Huelsmann, L., Geyer, T., Schweitzer, C., Priess, J., and Karthe, D.: The effect of subarctic conditions on water resources: initial results and limitations of the SWAT model applied to the Kharaa River Basin in Northern Mongolia, Environ. Earth Sci., 73, 581–592, https://doi.org/10.1007/s12665-014-3173-1, 2015.

Immerzeel, W. W., van Beek, L. P. H., and Bierkens, M. F. P.: Climate Change Will Affect the Asian Water Towers, Science, 328, 1382–1385, https://doi.org/10.1126/science.1183188, 2010.

IPCC: Climate Change 2021 – The Physical Science Basis: Working Group I Contribution to the Sixth Assessment Report of the Intergovernmental Panel on Climate Change, Cambridge University Press, Cambridge, 2021.

Ireson, A. M., van der Kamp, G., Ferguson, G., Nachshon, U., and Wheater, H. S.: Hydrogeological processes in seasonally frozen northern latitudes: understanding, gaps and challenges, Hydrogeol. J., 21, 53–66, https://doi.org/10.1007/s10040-012-0916-5, 2013.

Iwata, Y., Nemoto, M., Hasegawa, S., Yanai, Y., Kuwao, K., and Hirota, T.: Influence of rain, air temperature,

and snow cover on subsequent spring-snowmelt infiltration into thin frozen soil layer in northern Japan, J. Hydrol., 401, 165–176, https://doi.org/10.1016/j.jhydrol.2011.02.019, 2011.

Iwata, Y., Yanai, Y., Yazaki, T., and Hirota, T.: Effects of a snow-compaction treatment on soil freezing, snowmelt runoff, and soil nitrate movement: A field-scale paired-plot experiment, J. Hydrol., 567, 280–289, https://doi.org/10.1016/j.jhydrol.2018.10.016, 2018.

Jafarov, E. E., Coon, E. T., Harp, D. R., Wilson, C. J., Painter, S. L., Atchley, A. L., and Romanovsky, V. E.: Modeling the role of preferential snow accumulation in through talik development and hillslope groundwater flow in a transitional permafrost landscape, Environ. Res. Lett., 13, 105006, https://doi.org/10.1088/1748-9326/aadd30, 2018.

Kalantari, Z., Lyon, S. W., Jansson, P.-E., Stolte, J., French, H. K., Folkeson, L., and Sassner, M.: Modeller subjectivity and calibration impacts on hydrological model applications: An event-based comparison for a road-adjacent catchment in south-east Norway, Sci. Total Environ., 502, 315–329, https://doi.org/10.1016/j.scitotenv.2014.09.030, 2015.

Krysanova, V., Bronstert, A., and Muller-Wohlfeil, D. I.: Modelling river discharge for large drainage basins: from lumped to distributed approach, Hydrol. Sci. J.-J. Sci. Hydrol., 44, 313–331, https://doi.org/10.1080/02626669909492224, 1999.

Kurylyk, B. L.: Discussion of "A Simple Thaw-Freeze Algorithm for a Multi-Layered Soil using the Stefan Equation' by Xie and Gough (2013), Permafrost Periglacial Process., 26, 200–206, https://doi.org/10.1002/ppp.1834, 2015.

Li, C., Su, F., Yang, D., Tong, K., Meng, F., and Kan, B.: Spatiotemporal variation of snow cover over the Tibetan Plateau based on MODIS snow product, 2001-2014, Int. J. Climatol., 38, 708–728, https://doi.org/10.1002/joc.5204, 2018.

Li, X., Zhang, K., Niu, J., and Liu, L.: A machine learning-based dynamic ensemble selection algorithm for microwave retrieval of surface soil freeze/thaw: A case study across China, GIScience & Remote Sensing, 59, 1550–1569, https://doi.org/10.1080/15481603.2022.2122117, 2022.

Li, Z., Dong, Z., Liang, Z., and Yang, T.: Flood Forecast and Flood Management of large watershed, Water Power, 30, 12–15, 2004.

Li, Z., Xu, Z., and Li, Z.: Performance of WASMOD and SWAT on hydrological simulation in Yingluoxia watershed in northwest of China, Hydrol. Process., 25, 2001–2008, https://doi.org/10.1002/hyp.7944, 2011.

Liang, X., Lettenmaier, D., Wood, E., and Burges, S.: A Simple Hydrologically Based Model of Land-

Surface Water and Energy Fluxes for General-Circulation Models, J. Geophys. Res.-Atmos., 99, 14415–14428, https://doi.org/10.1029/94JD00483, 1994.

Liang, X., Wood, E. F., and Lettenmaier, D. P.: Surface soil moisture parameterization of the VIC-2L model: Evaluation and modification, Glob. Planet. Change, 13, 195–206, https://doi.org/10.1016/0921-8181(95)00046-1, 1996.

Maurer, G. E. and Bowling, D. R.: Seasonal snowpack characteristics influence soil temperature and water content at multiple scales in interior western US mountain ecosystems, Water Resour. Res., 50, 5216–5234, https://doi.org/10.1002/2013WR014452, 2014.

New, M., Hulme, M., and Jones, P.: Representing twentieth-century space-time climate variability. Part II: Development of 1901-96 monthly grids of terrestrial surface climate, J. Clim., 13, 2217–2238, https://doi.org/10.1175/1520-0442(2000)013<2217:RTCSTC>2.0.CO;2, 2000.

Peng, X., Zhang, T., Frauenfeld, O. W., Wang, K., Cao, B., Zhong, X., Su, H., and Mu, C.: Response of seasonal soil freeze depth to climate change across China, Cryosphere, 11, 1059–1073, https://doi.org/10.5194/tc-11-1059-2017, 2017.

Pomeroy, J. W., Gray, D. M., Brown, T., Hedstrom, N. R., Quinton, W. L., Granger, R. J., and Carey, S. K.: The cold regions hydrological process representation and model: a platform for basing model structure on physical evidence, Hydrol. Process., 21, 2650–2667, https://doi.org/10.1002/hyp.6787, 2007.

Potapov, P., Hansen, M. C., Pickens, A., Hernandez-Serna, A., Tyukavina, A., Turubanova, S., Zalles, V., Li, X., Khan, A., Stolle, F., Harris, N., Song, X.-P., Baggett, A., Kommareddy, I., and Kommareddy, A.: The Global 2000-2020 Land Cover and Land Use Change Dataset Derived from the Landsat Archive: First Results, Front. Remote Sens., 3, 856903, https://doi.org/10.3389/frsen.2022.856903, 2022.

Qi, J., Li, S., Li, Q., Xing, Z., Bourque, C. P.-A., and Meng, F.-R.: A new soil-temperature module for SWAT application in regions with seasonal snow cover, J. Hydrol., 538, 863–877, https://doi.org/10.1016/j.jhydrol.2016.05.003, 2016.

Qi, J., Wang, L., Zhou, J., Song, L., Li, X., and Zeng, T.: Coupled Snow and Frozen Ground Physics Improves Cold Region Hydrological Simulations: An Evaluation at the upper Yangtze River Basin (Tibetan Plateau), J. Geophys. Res.-Atmos., 124, 12985–13004, https://doi.org/10.1029/2019JD031622, 2019.

Ran, Y., Li, X., Cheng, G., Zhang, T., Wu, Q., Jin, H., and Jin, R.: Distribution of Permafrost in China: An Overview of Existing Permafrost Maps, Permafrost Periglacial Process., 23, 322–333, https://doi.org/10.1002/ppp.1756, 2012.

Ran, Y., Li, X., Cheng, G., Che, J., Aalto, J., Karjalainen, O., Hjort, J., Luoto, M., Jin, H., Obu, J., Hori, M., Yu, Q., and Chang, X.: New high-resolution estimates of the permafrost thermal state and hydrothermal conditions over the Northern Hemisphere, Earth Syst. Sci. Data, 14, 865–884, https://doi.org/10.5194/essd-14-865-2022, 2022.

Rush, M. J. and Rajaram, H.: Influence of Snowpack Cold Content on Seasonally Frozen Ground and Its Hydrologic Consequences: A Case Study From Niwot Ridge, CO, Water Resour. Res., 58, e2021WR031911, https://doi.org/10.1029/2021WR031911, 2022.

Shiklomanov, N. I.: Non-climatic factors and long-term, continental-scale changes in seasonally frozen ground, Environ. Res. Lett., 7, 011003, https://doi.org/10.1088/1748-9326/7/1/011003, 2012.

Song, L., Wang, L., Zhou, J., Luo, D., and Li, X.: Divergent runoff impacts of permafrost and seasonally frozen ground at a large river basin of Tibetan Plateau during 1960-2019, Environ. Res. Lett., 17, 124038, https://doi.org/10.1088/1748-9326/aca4eb, 2022.

Stephens, D. B.: Vadose Zone Hydrology, CRC Press, Boca Raton, Florida, 1996.

Streletskiy, D. A., Tananaev, N. I., Opel, T., Shiklomanov, N. I., Nyland, K. E., Streletskaya, I. D., Tokarev, I., and Shiklomanov, A. I.: Permafrost hydrology in changing climatic conditions: seasonal variability of stable isotope composition in rivers in discontinuous permafrost, Environ. Res. Lett., 10, 095003, https://doi.org/2020031315130486, 2015.

Thomas, H. R., Cleall, P., Li, Y.-C., Harris, C., and Kern-Luetschg, M.: Modelling of cryogenic processes in permafrost and seasonally frozen soils, Geotechnique, 59, 173–184, https://doi.org/10.1680/geot.2009.59.3.173, 2009.

U. S. Department of Algriculture: Soil survey manual, University Press of the Pacific, Forest Grove, Oregon, 2002.

Venäläinen, A., Tuomenvirta, H., Heikinheimo, M., Kellomäki, S., Peltola, H., Strandman, H., and Väisänen, H.: Impact of climate change on soil frost under snow cover in a forested landscape, Clim. Res., 17, 63–72, https://doi.org/10.3354/cr017063, 2001.

Walvoord, M. A., Voss, C. I., and Wellman, T. P.: Influence of permafrost distribution on groundwater flow in the context of climate-driven permafrost thaw: Example from Yukon Flats Basin, Alaska, United States, Water Resour. Res., 48, W07524, https://doi.org/10.1029/2011WR011595, 2012.

Walvoord, M. A., Voss, C. I., Ebel, B. A., and Minsley, B. J.: Development of perennial thaw zones in boreal hillslopes enhances potential mobilization of permafrost carbon, Environ. Res. Lett., 14, 015003,

https://doi.org/10.1088/1748-9326/aaf0cc, 2019.

Wang, G., Mao, T., Chang, J., Song, C., and Huang, K.: Processes of runoff generation operating during the spring and autumn seasons in a permafrost catchment on semi-arid plateaus, J. Hydrol., 550, 307–317, https://doi.org/10.1016/j.jhydrol.2017.05.020, 2017.

Wang, L., Koike, T., Yang, K., Jackson, T. J., Bindlish, R., and Yang, D.: Development of a distributed biosphere hydrological model and its evaluation with the Southern Great Plains Experiments (SGP97 and SGP99), J. Geophys. Res.-Atmos., 114, D08107, https://doi.org/10.1029/2008JD010800, 2009.

Wang, T., Yang, D., Fang, B., Yang, W., Qin, Y., and Wang, Y.: Data-driven mapping of the spatial distribution and potential changes of frozen ground over the Tibetan Plateau, Sci. Total Environ., 649, 515–525, https://doi.org/10.1016/j.scitotenv.2018.08.369, 2019.

Wang, X. and Chen, R.: Influence of snow cover on soil freeze depth across China, Geoderma, 428, 116195, https://doi.org/10.1016/j.geoderma.2022.116195, 2022.

Wu, N., Zhang, K., Chao, L., Ning, Z., Wang, S., and Jarsjö, J.: Snow cover expansion with contrasting depth thinning in the recent 40 years: Evidence from the Yalong River Basin, South-eastern Tibetan Plateau, J. Hydrol.-Reg. Stud., 53, 101786, https://doi.org/10.1016/j.ejrh.2024.101786, 2024.

Xie, C. and Gough, W. A.: A Simple Thaw-Freeze Algorithm for a Multi-Layered Soil using the Stefan Equation, Permafrost Periglacial Process., 24, 252–260, https://doi.org/10.1002/ppp.1770, 2013.

Yan, D., Ma, N., and Zhang, Y.: Development of a fine-resolution snow depth product based on the snow cover probability for the Tibetan Plateau: Validation and spatial-temporal analyses, J. Hydrol., 604, 127027, https://doi.org/10.1016/j.jhydrol.2021.127027, 2022.

Yang, D., Gao, B., Jiao, Y., Lei, H., Zhang, Y., Yang, H., and Cong, Z.: A distributed scheme developed for eco-hydrological modeling in the upper Heihe River, Sci. China-Earth Sci., 58, 36–45, https://doi.org/10.1007/s11430-014-5029-7, 2015.

Yao, C., Li, Z., Bao, H., and Yu, Z.: Application of a Developed Grid-Xinanjiang Model to Chinese Watersheds for Flood Forecasting Purpose, J. Hydrol. Eng., 14, 923–934, https://doi.org/10.1061/(ASCE)HE.1943-5584.0000067, 2009.

Yao, C., Li, Z., Yu, Z., and Zhang, K.: A priori parameter estimates for a distributed, grid-based Xinanjiang model using geographically based information, J. Hydrol., 468–469, 47–62, https://doi.org/10.1016/j.jhydrol.2012.08.025, 2012.

Yao, C., Zhang, K., Yu, Z., Li, Z., and Li, Q.: Improving the flood prediction capability of the Xinanjiang

model in ungauged nested catchments by coupling it with the geomorphologic instantaneous unit hydrograph, J. Hydrol., 517, 1035–1048, https://doi.org/10.1016/j.jhydrol.2014.06.037, 2014.

Yao, T., Bolch, T., Chen, D., Gao, J., Immerzeel, W., Piao, S., Su, F., Thompson, L., Wada, Y., Wang, L., Wang, T., Wu, G., Xu, B., Yang, W., Zhang, G., and Zhao, P.: The imbalance of the Asian water tower, Nat. Rev. Earth Environ., 3, 618–632, https://doi.org/10.1038/s43017-022-00299-4, 2022.

Yu, L., Zeng, Y., Wen, J., and Su, Z.: Liquid-Vapor-Air Flow in the Frozen Soil, J. Geophys. Res.-Atmos., 123, 7393–7415, https://doi.org/10.1029/2018JD028502, 2018.

Zhang, T., Barry, R. G., Knowles, K., Ling, F., and Armstrong, R. L.: Distribution of seasonally and perennially frozen ground in the Northern Hemisphere, in: Permafrost, Vols 1 and 2, 8th International Conference on Permafrost, Leiden, Web of Science ID: WOS:000185049300226, 1289–1294, 2003.

Zhang, Y., Cheng, G., Li, X., Jin, H., Yang, D., Flerchinger, G. N., Chang, X., Bense, V. F., Han, X., and Liang, J.: Influences of Frozen Ground and Climate Change on Hydrological Processes in an Alpine Watershed: A Case Study in the Upstream Area of the Hei'he River, Northwest China, Permafrost Periglacial Process., 28, 420–432, https://doi.org/10.1002/ppp.1928, 2017.

Zhao, R.: Hydrological simulation of watersheds, China Water Power Press, Beijing, 1984.

Zhao, R. and Wang, P.: Parameters analysis of Xin'anjiang model, Journal of China Hydrology, 8, 2–9, 1988.

Zou, D., Zhao, L., Wu, T., Wu, X., Pang, Q., and Wang, Z.: Modeling ground surface temperature by means of remote sensing data in high-altitude areas: test in the central Tibetan Plateau with application of moderate-resolution imaging spectroradiometer Terra/Aqua land surface temperature and ground-based infrared radiometer, J. Appl. Remote Sens., 8, 083516, https://doi.org/10.1117/1.JRS.8.083516, 2014.